

ABSTRACT

Title of Thesis: CHARACTERIZATION OF TRANSIENT
PRESSURE LOADS IN THE RESERVOIR OF
A HYPERSONIC BLOWDOWN TUNNEL

Kerrie Anne Smith, M.S., 2005

Thesis Directed By: Professor Mark J. Lewis, Department of
Aerospace Engineering

When flow through a hypersonic blowdown tunnel is initiated by the bursting of a diaphragm, expansion of the process gas into the downstream vacuum of the facility creates a strong rarefaction wave. This rarefaction propagates upstream, generating significant pressure drops in upstream components, such as a heater. These pressure drops can be attenuated with the use of a metering orifice, which requires an accurate prediction of the pressure drop for proper sizing. So as to be generally applicable and to provide physical insight, a closed-form or simple numerical solution for determining this pressure drop is preferred over computational fluid dynamics. Three methods are investigated: acoustic reflection, flow pattern assumption, and the Method of Characteristics. By examining the three methods in conjunction, tradeoffs between complexity and physical accuracy can be analyzed. Ultimately, this study shall lead to the design of an experiment to verify the accuracy of the three methods.

CHARACTERIZATION OF TRANSIENT PRESSURE LOADS IN THE
RESERVOIR OF A HYPERSONIC BLOWDOWN TUNNEL

By

Kerrie Anne Smith

Thesis submitted to the Faculty of the Graduate School of the
University of Maryland, College Park, in partial fulfillment
of the requirements for the degree of
Master of Science
2005

Advisory Committee:

Professor Mark J. Lewis, Chair
Associate Professor Kenneth Yu
Visiting Professor Robert Korkegi

© Copyright by
Kerrie Anne Smith
2005

ACKNOWLEDGEMENTS

I would like to thank my advisor, Dr. Mark Lewis, for his guidance and advice on this project, as well as throughout my graduate school experience. I would also like to extend thanks to Dr. Kenneth Yu and Dr. Robert Korkegi for serving on my committee.

Portions of this work have been supported by Arnold Engineering Development Center, with John Lafferty as technical monitor and by the Space Vehicle Technology Institute under grant NCC3-989 jointly funded by NASA and DOD within the NASA Constellation University Institutes Project, with Claudia Meyer as the project manager.

The staff of AEDC Hypervelocity Tunnel 9 have been invaluable. In addition to inspiring this research, they have been incredibly supportive and helpful in both my theoretical studies and the development of a validation experiment. In particular, I would like to thank Joe Coblish, as well as John Lafferty, Dan Marren and Joe Norris.

I would like to thank all the members of my research group for advice, opinions, and mutual sympathy.

Finally, I would like to thank my family and friends for all the love, support and enthusiasm they have given me during the last two years.

TABLE OF CONTENTS

ABSTRACT	
ACKNOWLEDGEMENTS	ii
TABLE OF CONTENTS	iii
LIST OF FIGURES	v
LIST OF ABBREVIATIONS	vi
1. Introduction	1
1.1. Motivation	1
1.2. Historical Overview of the Problem	3
1.3. Review of Existing Literature	5
1.3.1. Acoustic Reflection	5
1.3.2. Flow Pattern Assumption	6
1.3.3. Computational Analysis	7
2. Formation of the Model Problem	10
2.1. Unique Physical Features of the Flow	10
2.2. Characteristics of a Desirable Model	11
2.3. Model Geometry	12
3. The Acoustic Method	16
3.1. Description of the Method	16
3.2. Junction of Two Pipes	18
3.3. Junction of Three Pipes	20
3.4. Closed Pipes	21
3.5. Choke Point	22
3.6. Application to the Problem	22
4. The Flow Pattern Assumption Method	26
4.1. Description of the Method	26
4.2. The Basic Shock Tube Equations	26
4.3. Alpher and White's Method	29
4.4. Igra and Gottlieb's Method for Area Expansions	34
4.5. Gottlieb and Igra's Method for Area Contractions	38
4.6. Application to the Problem	41
5. The Method of Characteristics	46
5.1. Description of the Method	46
5.2. Derivation of Governing Equations	47
5.3. Application to the Problem	52
5.3.1. Set-Up	52
5.3.2. Internal Points	53
5.3.3. Boundaries	55
6. Results	61
6.1. Similarity	61
6.2. Comparison of Solutions	62
6.3. Application to Tunnel Design	76

6.4. Ablative Orifice	78
7. Design of Experiment	80
8. Conclusions.....	82
BIBLIOGRAPHY.....	86

LIST OF FIGURES

Fig. 2.1. Schematic of model tunnel.....	13
Fig. 3.1. Pressure pulse transmitted through two-pipe junction.....	18
Fig. 3.2. Pressure pulse transmitted through three-pipe junction.....	20
Fig. 3.3. Pressure pulse reflected off the end of the closed deck.	21
Fig. 3.4. Transmitted pressure to horizontal pipe vs. orifice restriction ratio for a variety of diaphragm pressure ratios.	24
Fig. 3.5. Pressure at top of heater vs. orifice restriction ratio for a variety of diaphragm pressure ratios.	24
Fig. 3.6. Pressure at bottom of heater vs. orifice restriction ratio for a variety of diaphragm pressure ratios.	25
Fig. 4.1. Constant area shock tube.	27
Fig. 4.2. Shock tube with area change at the diaphragm section.	29
Fig. 4.3. Flow pattern as a rarefaction encounters an increase in area.	35
Fig. 4.4. Subsonic flow pattern as a rarefaction encounters an increase in area.	39
Fig. 4.5. Results of flow pattern assumption methods.	43
Fig. 6.1. Pressure histories in horizontal pipe for $z=100$ and $z=100,000$ with $C=40\%$	61
Fig. 6.2. Pressure traces for $C=5\%$	66
Fig. 6.3. Pressure traces for $C=20\%$	67
Fig. 6.4. Pressure traces for $C=40\%$	68
Fig. 6.5. Pressure traces for $C=60\%$	69
Fig. 6.6. Pressure traces for $C=80\%$	70
Fig. 6.7. Pressure traces for $C=95\%$	71
Fig. 6.8. Comparison of pressure predictions between methods. a-b) Incident and reflected waves, horizontal. c-d) Incident and reflected waves, angled pipe. e-f) Incident and reflected waves, middle of heater. g) Top of heater. h) Bottom of heater.	75
Fig. 6.9. Pressure drop across the heater base.....	76
Fig. 6.10. Pressure traces in horizontal pipe for $C=.25$, $C=.45$ and a variable area orifice which expands from $C=.25$ to $C=.45$ over the first .01s (shown at axial midpoint of pipe).	78

LIST OF ABBREVIATIONS

A	Cross-sectional area
C	Constriction ratio
D	Diameter
L	Length
M	Mach number, differential operator along a minus characteristic
N	Differential operator along a plus characteristic, number of interior nodes
P	Pressure
R	Acoustic reflection coefficient, gas constant
S	Substantial derivative
T	Acoustic transmission coefficient
U	Volume velocity
Z	Acoustic impedance
a	Speed of sound
c_p	Specific heat at constant pressure
f	Frictional force at the wall per unit mass of fluid
h	Enthalpy
m	Riemann invariant along a minus characteristic
n	Riemann invariant along a plus characteristic
s	Entropy
t	Time
u	Particle velocity
x	Axial location

z	Initial diaphragm pressure ratio
β	Slope of a characteristic
γ	Ratio of specific heats
ρ	Density
θ	Random number
Subscripts	
0	Stagnation conditions, initial conditions
$1, 2, 3$	Physical location
$+,-$	From the positive or negative direction
i	Incident
$large$	Conditions in larger pipe of junction
max	Maximum
min	Conditions at minimum area
out	Outflow conditions
r	Reflected
ref	Reference
$small$	Conditions in smaller pipe of junction
t	Transmitted
Superscripts	
$*$	Sonic conditions
$'$	Non-dimensional

1. Introduction

1.1. Motivation

Hypersonic testing presents a number of unique challenges which make high Mach number facilities fundamentally different than their subsonic counterparts. Runtimes will be short; blowdown tunnels may run for as long as 10 to 15 seconds, but other types of tunnels may operate for only a few milliseconds. Flow is generally initiated through the bursting of diaphragms, making the run process less controllable than one governed by pumps and fans. Large volumes of test gas will need to be stored at extremely high pressures and temperatures.

Despite the operational difficulties, hypersonic tunnels are critical for expanding the limits of high-speed flight. Through hypersonic testing, new ballistic missile subsystems, such as shroud separation and optical tracking can be developed. Research can be conducted towards advanced propulsion methods, such as ram- and scramjets. Simulation of re-entry flows permits testing of vehicles like the Apollo capsule or the space shuttle. Basic research flows can be investigated to further understanding of hypervelocity physics, such as boundary layers and viscous interactions.

Providing sufficient enthalpy is critical for achieving hypersonic conditions in a high-speed wind tunnel. One approach is the use of a heater. This heater must transfer sufficient energy to the working fluid to prevent condensation during the expansion into the test section, while withstanding the high pressures necessary to provide hypersonic flow. Generally, in wind tunnel analysis of downstream components, such as the test section, the heater is treated as a theoretical reservoir, i.e., at pressure conditions.

However, during the start-up process of the tunnel, prior to the establishment of steady flow, the heater may encounter a transient pressure drop. This pressure drop can be detrimental for a number of reasons. Many wind tunnel heaters function by forcing the air through a bed of hot refractory pebbles. A pressure drop across the bed lifts the pebbles, drawing them out of the heater and into the test section. Pressure drop is considered to be the most critical parameter in design of a pebble-bed heater.²⁵ In facilities where batch heating is used, the pressure vessel must be insulated from the extreme test gas temperatures required for hypersonic flow establishment. Protective liners may be inserted into the heater so that it may operate at temperatures higher than the yield of the pressure vessel material. In this case, pressure differences on either side of the liner can cause it to collapse during the startup process. Finally, in resistance heaters, the heating elements themselves may be delicate, and sensitive to changes in pressure and temperature.

Engineering around these problems is not generally difficult. Liners can be designed to withstand the maximum pressure difference. Metering orifices can be added to the flow paths to choke the flow, and thus decrease the magnitude of the effective pressure gradient downstream of the reservoir. However, in both these cases, an accurate estimate of the magnitude of the pressure drop is required. Furthermore, a testing facility may change the conditions of the tunnel with every run, meaning that either the heater must be over-designed to meet the most stringent conditions that may be experienced, or more practically, interchangeable orifices may be used. If the latter is the case, an analytic or very simple computational pressure drop model would be preferred over the use of computational fluid dynamics. Moreover, an analytic solution would provide more

insight into the essential physics of the problem, perhaps leading to alternate or improved protective measures.

1.2. Historical Overview of the Problem

Wind tunnels have been an indispensable tool in the study of aerodynamics for over a century. Although early aerodynamicists used natural winds and whirling arm mechanisms starting in the 1600's,⁴² the first true wind tunnel was built in 1871, in England, by Frank H. Wenham.³ Only 30 years later, in 1899, a Frenchman named Paul Vieille published a design for a shock tube wind tunnel capable of supersonic speeds. Based on the mathematical work of Riemann, the shock tube consisted of a cylinder in which a high pressure region was separated from a low pressure region by a diaphragm. Upon instantaneous removal of the diaphragm, the high-pressure fluid was accelerated toward the low-pressure end of the tube. The initial pressure ratio across the diaphragms determined the maximum velocity of the fluid. Vieille's design was able to reach flow velocities of 600 m/s by expanding pressurized air from 27 atm to atmospheric pressure, using a collodion diaphragm. Unfortunately, little was done with his work until the 1920's, when Payman and Shepherd at the Safety in Mines Research Board in England used a Schlieren system to study shock waves from solid detonators, gaseous explosions, and around bullets. Because of World War II, their work could not be published until 1946.¹¹ The Germans carried out simultaneous work with significantly more success: when the Allies captured the V-2 testing facility, they discovered a tunnel capable of attaining Mach 5 flow and a Mach 10 tunnel in construction⁵. After the war, shock tube technology developed quickly, and came into use at Princeton, Cornell, Toronto, and later, other universities and research centers around the world.¹¹

In the 1950's, interest arose over the use of area changes and orifices for the purpose of conditioning wind tunnel flow. It was theorized by Resler, Lin and Kantrowitz that an area decrease in the diaphragm section could generate a stronger shock for the same diaphragm pressure ratio. This was explored theoretically and experimentally by Alpher and White¹. At the Tenth International Shock Tube Symposium, held in Kyoto in 1975, Barbour and Imrie⁶ proposed that an orifice placed at the entrance to the reservoir of a Ludwieg tube (a shock tube with a very long high-pressure section to act like the reservoir of a blowdown tunnel) could extend the run time of the tunnel without increasing the length of the storage tube. They hoped to tailor the orifice size so that the rarefaction downstream of the orifice would cancel the reflected expansion wave from the downstream boundary of the test section, which would normally end useful test time upon reaching the nozzle. Similarly motivated, Matsuo, Kawagoe and Ogawara²⁶ presented work at the same conference on extending test time by replacing the traditional diaphragms with a rapid-opening valve. Inspired by Barbour and Imrie's work, Matsuo and Kawagoe went on to publish a number of other papers investigating the starting²⁸ and choking²⁷ processes of tunnels containing area constrictions. They also investigated the extension of steady flow time via an orifice²⁹, especially one whose open area could vary through the use of valves or ablatives³⁰. An important side benefit of orifice use is that, due to choking of the flow, pressure gradients behind the orifice are greatly reduced.

An alternate method found to increase shock strength was addition of heat to the reservoir gas, a technique that could be combined with area contractions for maximum effect³⁴. Heating the test gas functions by increasing the speed of sound in the driver gas as well as the enthalpy of the fluid. Without sufficient enthalpy, the gas could liquefy as it

expands in the test section. However, storing gas at the extreme temperatures and pressures necessary to generate hypersonic flow could cause damage to a heater tank. In 1975, the NASA Ames 3.5 foot hypersonic tunnel, made of 8-inch thick steel plate, suffered catastrophic flange failure. The pressurized gas and red-hot refractory pebbles shooting forth from the rupture caused several fires and significant damage to the tunnel building; fortunately, no one was hurt.⁵ Although this was a rare incident, it emphasizes the importance of limiting the transient loading on the heater vessel as much as possible, since it is already severely stressed by heat and pressure. Orifices are an excellent way of protecting against such gradients, and they impart many other performance benefits as well.

1.3. Review of Existing Literature

In this work, three methods of analyzing hypersonic fluid flow through a number of area changes are investigated. Each carries with it a body of existing literature, which will be reviewed briefly.

1.3.1. Acoustic Reflection

The first method employed is based on transient propagation theory, designed for handling pressure surge in pipes. The first work on water hammer was published in 1865 by Ernst Weber, a physician interested in the flow of blood through the circulatory system. Throughout the mid-1800's, scientists studied propagation of waves in pipes, and role that pipe elasticity plays in changing the speed of sound of the medium. An important contribution to the field came when the Moscow Water Works undertook a comprehensive study, published in 1900 by Joukowsky. This report was the first to

recognize the relationship between surge pressure (or pressure head) and change in velocity. It also introduced the importance of wave reflections and speed of sound through the concept of a pipe period, the time it takes for a wave to reach a boundary and return. Similar work was being done by an American, J. P. Frizell, at the same time. Allevi, an Italian researcher, used Joukowsky's results to derive a general method for flow through a frictionless, homogenous pipe with a uniform velocity distribution. He extended the work to include slow valve closures and to calculate pressure at any point in a pipe, instead of only at boundaries. Methods were added to account for friction and longitudinal stresses, but after 1913, pressure surge methods would remain almost unchanged until the advent of digital computers⁴¹.

1.3.2. Flow Pattern Assumption

The second method considered in this paper was developed primarily for shock tubes. In the early 1950's, experiments showed a shock tube with an area decrease at the diaphragm section could produce a stronger shock from the same initial diaphragm pressure ratio than a tube of constant area. The most famous analysis of such a case was published by Alpher and White in 1958¹. Alpher and White posited that a characteristic pattern of shock and expansion waves would occur in such a situation, which could be solved to determine pressure at any point in the tube. Hall and Russo¹⁴ later proposed a simplification to these equations for high Mach numbers. An experimental study was made by Sugiyama⁴⁰ to verify Alpher and White's results, as well as explore the effects of diaphragm location, area ratio and the exact geometry of the convergent section. Their results showed agreement within about 7% of Alpher and White's.

In 1983, Igra and Gottlieb generalized Alpher and White's results to the scenario of an existing wave approaching an area change. They compared their results to a fully unsteady numerical solution utilizing the Random Choice Method to show that the initially unsteady solution converged to the quasi-steady solution, and to establish a characteristic convergence time. They found that the characteristic time increased with the strength of the incident rarefaction, and that it was only weakly dependent on the area ratio. A later paper by Igra, Wang and Falcovitz¹⁷ compared the results of the one-dimensional, quasi-steady analysis to a fully unsteady, two-dimensional numerical code.

1.3.3. Computational Analysis

In many cases, a highly accurate solution with good spatial and temporal resolution is desired, requiring a computational solution. There have been a number of computational studies regarding the start-up modes of shock tubes and tunnels. In general, flows through complex geometries are investigated both computationally and experimentally, bypassing analytical methods entirely. Lee,²³ used a Godunov scheme to compute the unsteady shock structure formed immediately upstream of a shock tube nozzle. Kaneko and Nakamura¹⁹ used a finite volume code to solve a similar problem for temperature. Results from both studies could be compared to the pattern observed experimentally by Amann in 1969². Jacobs¹⁸ also used a finite volume method in his investigation of frequency-focusing in expansion tubes, a topic which was studied experimentally by Paull and Stalker.³³ In the wave-propagation problem of interest to this study, however, there are two relatively simple computational schemes which are commonly utilized: the Method of Characteristics and the Random Choice Method.

The Method of Characteristics is a general procedure first proposed by Riemann in 1860 for obtaining exact solutions to hyperbolic partial differential equations. In this method, one constructs lines across the region of interest along which the PDE can be reduced to an ODE. In some special cases, it can be reduced to an algebraic expression. Although it is somewhat tedious, the Method of Characteristics can be performed graphically, which is how it was utilized for the following century. The method was first applied to supersonic flow in 1929 by Prandtl and Busemann³, and to analyze pressure transients in 1947 by Lamoen, although work by Gray in the mid-1950's received more attention. In 1960, Lister proposed an algorithm through which the Method of Characteristics could be implemented on a digital computer. Over the next forty years, it became a widely-used tool in the field of aerodynamics and in transient pipe flow⁴¹. This method has been covered in detail for a variety of applications in a number of textbooks, such as References 3, 10, 22, 31, 37 and 41.

The Random Choice Method is a much newer method, based on a proof by Glimm, and developed into a computational scheme by Chorin in 1976⁹. It was later improved through implementation of an operator-splitting method by Sod³⁹. This method has been used by a number of authors to solve shock tube start-up problems.^{20,32,38} The Random Choice Method solves a Riemann problem with boundaries at x and $x+\Delta x$. The Riemann solution consists of four regions separated by a left-running wave, a contact surface (which can run to the right or left) and a right-running wave. One wave will be a shock, but the other will be a rarefaction, and therefore, there is a fifth region inside the wave itself. A random number $-1/2 < \theta < 1/2$ is generated, and the solution at $(x+\Delta x/2, t+ \Delta t/2)$ is taken to be the solution to the Riemann problem at $(x+\theta\Delta x, t+ \Delta t/2)$. The main

advantage to the Random Choice Method is that it maintains the discontinuous nature of the shock, and thus has been found to capture sharp shock fronts with good time resolution. However, it is limited to a one-dimensional approximation, and furthermore, its accuracy in continuous waves (such as rarefactions) is not as refined as other methods. A higher-order random choice scheme was developed by Toro, but it could not retain the sharp shock solutions of the original method. Toro later suggested a hybrid method between the traditional and higher-order versions which would provide high accuracy in smooth regions while retaining sharp discontinuities.⁴²

Both the Method of Characteristics and the RCM offer similar advantages over the previous quasi-steady methods. They provide a time-dependent solution to which friction and entropy effects can be applied or neglected at the user's choosing. Boundary conditions based on geometric changes-- the most vital aspect of a computational solution to this particular problem-- would be implemented nearly identically for both cases. In short, it does not really matter which method is utilized, and applying both would not supply additional insight to the problem. The Method of Characteristics has been selected because it is much simpler to code, and because the capacity for a two-dimensional, unsteady analysis exists (although it is beyond the scope of this paper.) The strengths of Random Choice lie in shock resolution, which is not a critical issue in this particular application. Nevertheless, RCM has been used successfully in similar problems, and the interested reader is referred to the extensive work of Gottlieb, Igra and Murty.^{16,17,32}

2. Formation of the Model Problem

2.1. Unique Physical Features of the Flow

It is important to identify the physical parameters which may contribute significantly to the magnitude of the pressure drop in a heater. This will give a preliminary clue as to whether or not a given model will be useful and relevant. This problem exists outside of the regime where many simplifying idealized assumptions are valid. Nevertheless, these assumptions may still be incorporated into various solutions for the sake of simplicity. By using a combination of models which incorporate different assumptions in a systematic manner, one can see the effect of these assumptions on the overall solution. It is possible that many of the assumptions cannot be made, and certain solutions must be discarded or altered accordingly. However, a simple method may fortuitously provide an accurate answer if the parameter on which the poor assumption was made does not have a large impact on the solution. By starting with simple solutions, and adding detail until an acceptable solution can be found, either a relatively straightforward solution may be obtained, or a compelling argument can be made for the necessity of a highly-detail computation solution.

The first unique aspect of this flow is the extreme pressure ratios involved. Much of the literature on shock tubes considers diaphragm pressure ratios on the orders 10^0 - 10^4 .^{1,8,40} In pipe-flow problems, the pressure ratios are generally even smaller than that. However, pressure ratios on the order of 10^6 are necessary to generate hypersonic flows. Alpher and White state that above pressure ratios of 1000, ideal theory can no longer accurately predict shock tunnel flow, possibly due to combinations of imperfect

diaphragm rupture, mixing effects, shocked gas non-ideality and wall attenuation¹, but they do not indicate the magnitude of the resulting inaccuracy.

Secondly, gas within the heater vessel is maintained at extremely high temperature, often at thousands of degrees Kelvin. Gas can not be treated as ideal or calorically perfect at such temperatures. Therefore, the ratio of specific heats is not constant, and the ideal gas law is invalid.

The flow will be unsteady, i.e., dependent on time. It is believed that the peak pressure drop will occur in the transient flow regime before steady flow is established in the tunnel. Many treatments of flow through an area change, such as nozzle flow, assume that the flow is steady.

Finally, the problem contains a number of area changes, all of which should be treated as discontinuous. Many methods assume the area change gradual enough to be isentropic, i.e., that no separation occurs at area changes. Here, the area changes are not gradual, and separation is likely. *Vena contracta* formation is also probable, meaning that cross-sectional area of the flow will be smaller than the cross-sectional area of the pipe.

2.2. Characteristics of a Desirable Model

Obviously, the most desirable aspect of any mathematical model is accuracy. However, there are a number of other priorities to be considered. The first, as previously noted, is simplicity. The overall goal of this project is to generate a method which can be used to produce quick solutions for a wind tunnel of any geometry. To this end, the model should be in some part modular, i.e., each geometric feature will be treated as individual analysis within a series, instead of as a holistic system. This aspect of the model will make it easier to translate from one tunnel to another, where one may contain

an additional area change or reverse the order of a junction and an area change. In addition, this feature will make it easy to evaluate how changes in each section or alternate methods of modeling the flow through each section affect the solution as a whole. To further simplify the solution, it should take the form of either an analytic solution, or a swift-running computational solution with a minimum number of necessary inputs. Next, non-dimensionality is preferred to decrease the number of necessary verification tests as well as increasing the applicability of a given solution. Finally, the solution should account for all the physical flow features which are relevant to the problem, outlined in the previous section. Overall, the ideal solution is as simple and as general as possible within acceptable accuracy.

2.3. Model Geometry

Although an analysis of the flow through the heater of a specific test facility could be performed using CFD, the goal of this investigation is to develop a general engineering method that could be applied to any wind tunnel. Therefore, a generic "model heater" has been defined, representative of existing facilities. The model heater, pictured in Fig. 2.1, contains as many relevant area changes as possible. These features can be rearranged or omitted as necessary for a heater of different geometry. This particular configuration shall be used throughout the investigation as a means of comparing the efficacies of the various methods explored.

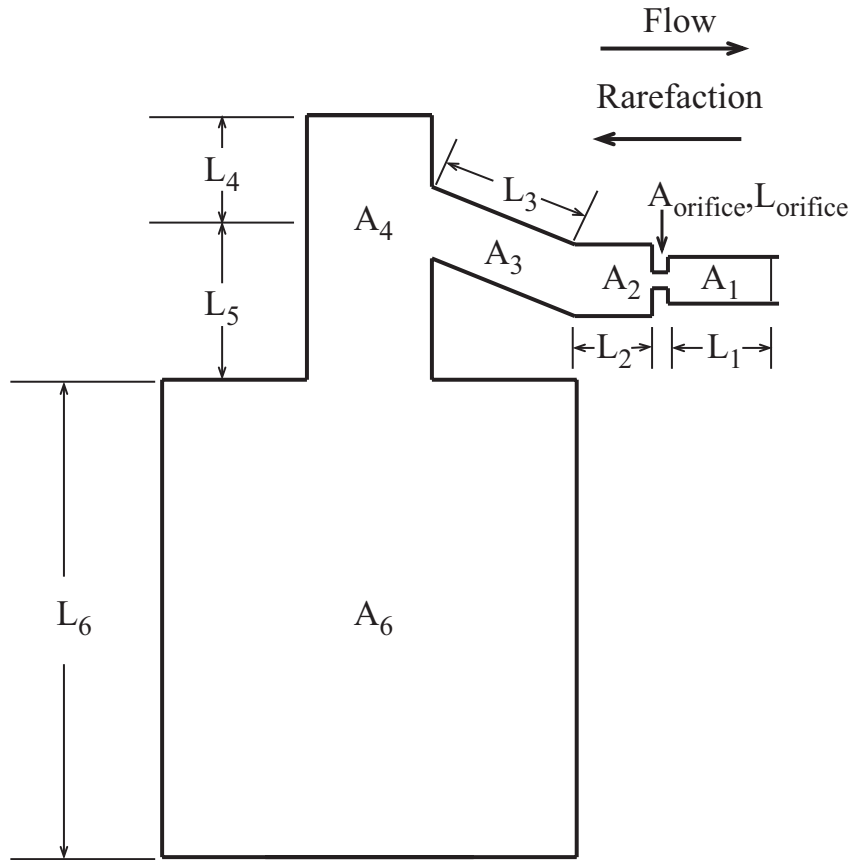


Fig. 2.1. Schematic of model tunnel.

In the model, as with the standard convention, flow moves from left to right, but the rarefaction wave propagates from right to left. The positive direction shall be taken with the rarefaction motion, meaning that the flow velocity will be negative. The diaphragms initially separate a high pressure region on the left from a low pressure region on the right. These two regions may or may not contain the same fluid, and thus ρ, γ and T may differ. Diaphragm rupture is assumed to be perfect. A wave is generated as the diaphragm is burst, and immediately begins to travel through a horizontal pipe of area A_1 . The distance between the diaphragm and the orifice is L_1 . The next region is a metering orifice of length $L_{orifice}$: a plate with a small effective area, used to reduce the pressure

drop to the heater by choking the flow to Mach 1. This effective area may be accomplished by a single hole in the middle of the plate, or an array of holes. For the purposes of this work, it will be assumed that one can generate a quantity representing the effective area, $A_{orifice}$, indicating equivalent performance to that of an orifice with a single hole of that area. Upstream of the orifice, the diameter of the tunnel increases to A_2 for a distance of L_2 where $A_2 > A_1$. Many tunnels contain such an area change, because it has been shown to increase the strength of the generated shock for a given initial pressure ratio.¹ Next, an angled pipe, area A_3 and length L_3 is included, because the reservoir may not be located in-line with the rest of the tunnel. Note that L_3 is taken as the length parallel to the axis of the pipe, not horizontally. The pipe could be angled up, down or to the side. Since the analyses presented here are one-dimensional, the angle itself does not affect the flow. Instead, the angled pipe is included because in order to have a mitered joint with the horizontal pipe, $A_3 < A_2$, which demonstrates the possible need for an area reduction. The angled pipe enters the top of the heater, a vertical pipe of area A_4 . A length L_4 of the heater lies above the angled pipe, and L_5 lies below. $A_4 = A_5$, for simplicity. The pipe below the angled pipe junction then connects to the largest portion of the reservoir with area A_6 and length L_6 .

In order to meaningfully compare the various methods explored in this study, values have been assigned to the areas and lengths. This is the equivalent of selecting a pre-existing wind tunnel and analyzing the pressure drop for a variety of orifices and run conditions. Different dimensions could be substituted if one were to apply these methods to a particular facility. For the purposes of this study, all cross-sections are assumed to be circular, of diameters $D_1=0.25$, $D_2=0.275$, $D_3=0.271$, $D_4=0.375$ and $D_5=1.25$ (all units are

meters). These correspond to $A_1=0.0491$, $A_2=0.0594$, $A_3=0.0576$, $A_4=0.110$ and $A_6=1.227$ respectively. The lengths are $L_1=1$, $L_2=0.5$, $L_3=2$, $L_4=.5$, $L_5=1$, $L_6=2$ and $L_{orifice}=0.1$. These dimensions are not based on any particular existing facility, but are realistic, representative values. $A_{orifice}$ has not been set; orifice size shall be treated as a variable, so behavior can be qualified as a function of orifice geometry. In fact, a new non-dimensional parameter, constriction ratio C , shall be introduced, where

$$C \equiv \frac{A_{orifice}}{A_1} \quad (1)$$

Note that in a statement such as "constriction ratio of 40%", it is implied that the orifice is constricted *to* 40% of the pipe area, not constricted *by* 40%. The other variable is the initial diaphragm pressure ratio, the ratio of the high pressure initially upstream of the diaphragms (which will also be the stagnation pressure) to the low pressure downstream of the diaphragms. As in Alpher and White, initial diaphragm pressure ratio shall be designated z .

3. The Acoustic Method

3.1. Description of the Method

The first method to be considered is the traditional acoustic transmission technique, commonly used in the treatment of transient conditions on networks of pipes^{15,21,41}. This method hinges on two major assumptions which may initially seem questionable for this application. The first is that the waves are linear, and therefore subject to the principle of superposition. In this manner, the baseline pressure is subtracted off entirely, and only perturbation pressures are dealt with. Secondly, it is assumed that the pressure pulse is small compared to the baseline pressure, implying that density and speed of sound of the fluid are not affected by the pulse. Since the pressure pulses in question are rarefactions, this is categorically false. However, it is unknown how severely this assumption will affect the results of the problem, so it will be retained with caution, and by comparing the predictions to those gained from more physically germane methods the effect of compressibility on the solution can be better quantified.

In this method, an incident pressure pulse of magnitude P_i is imposed onto the steady state conditions of the pipe. This pulse travels through the pipe until it meets a boundary: either a junction with one or more pipes, a valve, a reservoir, or a dead end. Acoustic theory considers a wide variety of such boundaries; in this paper, only conditions likely to be seen in a blowdown tunnel will be considered.

In this method, when a pressure transient encounters a boundary, a portion of the wave is transmitted, and a portion is reflected. The respective magnitudes of the incident, reflected and transmitted waves can be calculated by imposing the conditions that

pressure and volume velocity must be continuous at the junction. To this end, it is useful to calculate the impedance of each pipe, denoted by Z , defined as the ratio of the pressure to volume velocity,

$$Z = \frac{P}{U} = \frac{P}{uA} \quad (2)$$

where u is particle velocity (the velocity of a differential element of fluid) and A is the cross sectional area of the pipe. Impedance plays the same role in a fluid system as resistance in an electrical system. The impedance can also be calculated as a property of a fluid-filled pipe, equal to

$$\begin{aligned} Z_+ &= \frac{\rho a}{A} \\ Z_- &= -\frac{\rho a}{A} \end{aligned} \quad (3)$$

for waves propagating in the positive and negative directions, respectively. For this study, the left is considered to be the positive direction.

Since this is a non-dimensional approach, a coefficient of reflection and a coefficient of transmission shall be calculated at each boundary, defined such that

$$\begin{aligned} R &= \frac{P_r}{P_i} \\ T &= \frac{P_t}{P_i} = \frac{P_i + P_r}{P_i} = 1 + R \end{aligned} \quad (4)$$

As mentioned before, the pressure transients P_i , P_r and P_t are superimposed onto the steady-state reservoir pressure, P_0 , which is also the stagnation pressure. Since this

problem deals with rarefactions, the default sign for all three will be negative, meaning that the pulse decreases the baseline pressure. This has no bearing on the derivation, especially since pressures are often expressed as ratios of each other. The problem will be further non-dimensionalized by taking P_i , P_r and P_t to be normalized by P_0 . Therefore, P_i entering the first pipe will actually be the initial diaphragm pressure ratio, and the pressure at some point through which the pulse has already passed will be $P_0(1-P_i)$. The pressure at some point in the second pipe to the right of the wavefront will be $P_0(1-T_1P_i)$, in the third pipe, $P_0(1-T_1T_1T_2P_i)$, etc. To the left of a reflected wavefront, the pressure will be $P_0(1+P_i[R-1])$. The pressure will take on oscillatory behavior as reflected waves encounter downstream boundaries and re-reflect, so that waves are traveling both upstream and downstream simultaneously. A computational program could be written to model such behavior, but for the purposes of this investigation, the major concern is the maximum pressure drop which will be caused by the initial transmitted wave (as reflected waves will serve to attenuate the pressure drop). Therefore, only the initial transmission coefficients are considered important.

3.2. Junction of Two Pipes

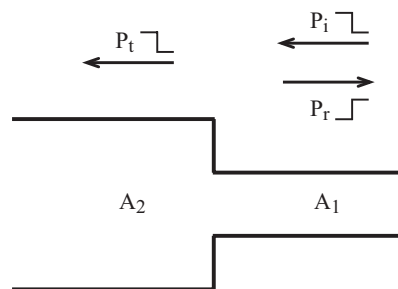


Fig. 3.1. Pressure pulse transmitted through two-pipe junction.

A junction of two pipes of impedance Z_1 and Z_2 is shown in Fig. 3.1. A_2 is shown to be bigger than A_1 , but this derivation applies to the opposite case, as well. The incoming wave, propagating from right to left, will be of magnitude P_i . The transmitted pressure drop will be P_t and the reflected pressure increase will be of magnitude P_r . (If $P_r < 0$, the reflected wave will be an expansion instead of a compression). Enforcing continuity of pressure at the boundary,

$$P_i + P_r = P_t \quad (5)$$

Enforcing continuity of velocity,

$$U_i + U_r = U_t \quad (6)$$

Dividing (5) by (6)

$$\frac{P_i + P_r}{U_i + U_r} = \frac{P_t}{U_t} \quad (7)$$

Substituting the definition of the impedance from Eq. (2)

$$\frac{P_i + P_r}{P_i / Z_i + P_r / Z_r} = Z_t = \frac{(P_i + P_r)A_1}{\rho_1 a_1 (P_i - P_r)} = \frac{\rho_2 a_2}{A_2} \quad (8)$$

Solving for P_r/P_i ,

$$R = \frac{P_r}{P_i} = \frac{1 - Z_t / Z_i}{Z_t / Z_r - 1} = \frac{\rho_2 a_2 A_1 / \rho_1 a_1 A_2 - 1}{\rho_2 a_2 A_1 / \rho_1 a_1 A_2 + 1} \quad (9)$$

In this particular problem, gas conditions do not change between pipes, so density and speed of sound will be the same for all three waves. Therefore, R is a function of the area ratio only:

$$R = \frac{A_1 - A_2}{A_1 + A_2} \quad (10)$$

3.3. Junction of Three Pipes

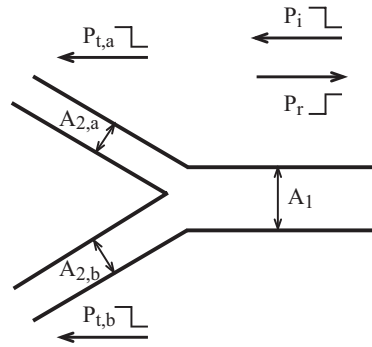


Fig. 3.2. Pressure pulse transmitted through three-pipe junction.

A three-pipe junction is treated exactly as a two pipe junction, except that there are two transmitted pressure pulses (of magnitudes $P_{t,a}$ and $P_{t,b}$ respectively) instead of one. As before, pressure is constant and particle velocity is conserved at the junction, so, analogous to Eq. (7)

$$\frac{P_i + P_r}{U_i + U_r} = \frac{P_{t,a}}{U_{t,a} + U_{t,b}} = \frac{P_{t,b}}{U_{t,a} + U_{t,b}} \quad (11)$$

Substituting $Z=P/u$,

$$\frac{\frac{P_i + P_r}{Z_i} + \frac{P_r}{Z_r}}{\frac{P_i + P_r}{Z_i} + \frac{P_r}{Z_r}} = \frac{1}{\frac{1}{Z_{t,a}} + \frac{1}{Z_{t,b}}} = \frac{\rho_1 a_1}{A_1} \frac{P_i + P_r}{P_i - P_r} = \frac{1}{\frac{A_a}{\rho_2 a_2} + \frac{A_b}{\rho_2 a_2}} = \frac{\rho_2 a_2}{A_a + A_b} \quad (12)$$

The reflection coefficient can then be solved for, as before, assuming that density and speed of sound are the same throughout the system:

$$R = \frac{A_1 - (A_a + A_b)}{A_1 + A_a + A_b} \quad (13)$$

Note that this is exactly the same result as the two pipe junction, where A_2 is replaced with $A_a + A_b$. From Eq. (11) it can be seen that $T_a = T_b = 1 + R$.

3.4. Closed Pipes

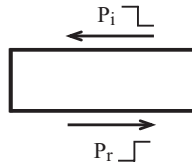


Fig. 3.3. Pressure pulse reflected off the end of the closed deck.

This case involves only an incident and a reflected wave. The only boundary condition that is necessary is the fact that the particle velocity at the dead end will be zero.

$$U_r + U_i = 0 = \frac{P_r}{Z_r} + \frac{P_i}{Z_i} \quad (14)$$

The reflection coefficient can be easily solved for.

$$R = \frac{P_r}{P_i} = \frac{-Z_i}{Z_r} = \frac{-\rho_1 a_1}{-\rho_1 a_1} = 1 \quad (15)$$

3.5. Choke Point

One final boundary condition is necessary, which does not come from acoustic theory, but rather from recognizing that if the pressure ratio is strong enough the flow will choke at the minimum cross-sectional area, which is the orifice. Acoustic theory in itself contains no mechanism for choking, so it must be accounted for explicitly. Given an isentropic flow, the ratio of stagnation pressure to sonic point pressure is given by

$$\frac{P^*}{P_0} = \left(\frac{2}{\gamma + 1} \right)^{\frac{\gamma}{\gamma - 1}} = 1 - P_{t,max} \quad (16)$$

This gives a maximum pressure drop which can be transmitted through the orifice. If $P_t > P_{t,max}$, then the pressure transmitted through the orifice is $P_{t,max}$, and P_t is irrelevant to the problem because no further pressure drop can be propagated upstream. For a hypersonic tunnel, P_t will unequivocally exceed $P_{t,max}$, so choking at the orifice is virtually guaranteed.

3.6. Application to the Problem

The application of the acoustic method is extremely straightforward; in fact, the equations are so simple that it can be implemented by hand. A given initial diaphragm pressure ratio, z , corresponds to an acoustic pulse of amplitude $P_t = 1 - z$. At an area change, R and T are calculated. The pressure wave transmitted through the junction, $P_t = T(1 - z)$ will be the initial pressure wave for the next junction. The pressure in pipe i normalized by the stagnation pressure is given by

$$P / P_0 = 1 - (1 - z) \prod_{n=1..i} (T_n) \quad (17)$$

For a reflected wave, such as off the top or bottom of the heater tank,

$$P / P_0 = 1 - (1 + R_i)(1 - z) \prod_{n=1..i} (T_n) \quad (18)$$

where R and T for each pipe are determined using the correct type of junction.

If the orifice is assumed to be choked, the orifice becomes Pipe 1, and $P_{t,max}$ replaces z as discussed in the previous section. As a consequence, if the choked condition is imposed, the transmitted pressures are independent of z and become a function of constriction ratio, C only. Fig. 3.4 shows the effect on the pressure just upstream of the orifice of imposing the choking condition as opposed to computing the orifice as two area junctions. It can be seen that as the pressure ratio increases, the transmitted pressure ratio reaches a limiting curve, and thus, independence of z arises regardless of whether choking is imposed or not. However, without the choking condition, the transmitted pressure drop is far larger than for the choked case, even for relatively small values of z . Since the pressure drop prediction in each pipe depends on the prediction in all the downstream pipes, these discrepancies will be propagated to all upstream pipes. Figures 3.4 and 3.5 show the pressure drop entering the top and bottom of the model heater. It is now obvious that the imposed choke condition is absolutely necessary in order to utilize this method. Also, recall that there are doubts regarding the assumption that the perturbation pressure would not affect the density and speed of sound of the medium. Other methods must be considered in order to determine the accuracy of this technique.

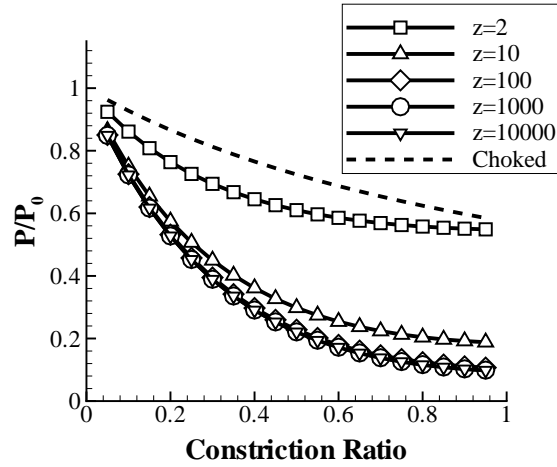


Fig. 3.4. Transmitted pressure to horizontal pipe vs. orifice restriction ratio for a variety of diaphragm pressure ratios.

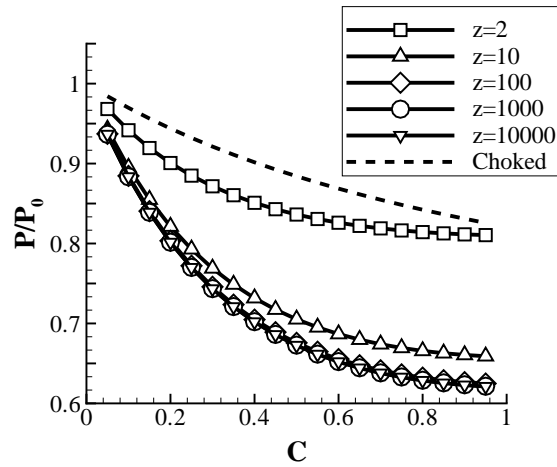


Fig. 3.5. Pressure at top of heater vs. orifice restriction ratio for a variety of diaphragm pressure ratios.

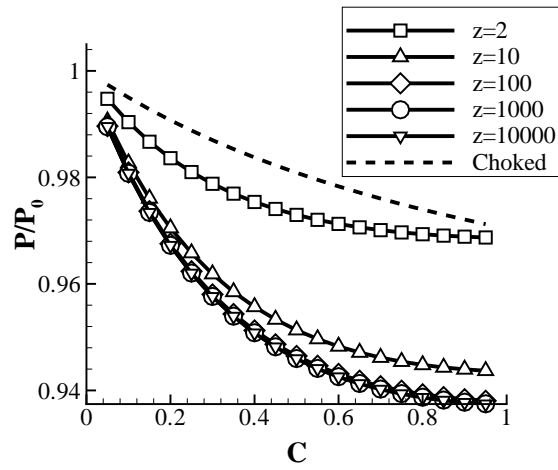


Fig. 3.6. Pressure at bottom of heater vs. orifice restriction ratio for a variety of diaphragm pressure ratios.

4. The Flow Pattern Assumption Method

4.1. Description of the Method

In the previous method, pressure waves passing through geometry changes have been treated as transmitted and reflected waves which can be superposed. However, at hypersonic speeds, pressure waves will behave nonlinearly, fanning out as expansion waves or coalescing into shocks. More restrictions must be placed on the flow to assure that it manifests itself in a way that is physically realizable. The following technique has been developed primarily for shock tubes. Although shock tubes lack a fluid reservoir, they are otherwise very similar to blowdown tunnels and commonly contain an area decrease downstream of the diaphragms, to strengthen the induced shock.

In the method which follows, a flow pattern is constructed of shock and expansion waves. Quasi-steady expressions are used to relate fluid properties across these waves. analytically determining the properties in any region of the tube. First, the simple case of a constant area shock tube will be reviewed. This case will be the basis of the analysis of an area change near the diaphragm region, and for an area change further upstream. Complicating the geometry of the shock tube through the addition of area changes adds more equations to the system, but does not change the underlying technique.

4.2. The Basic Shock Tube Equations

Examining the case of a constant area shock tube develops most of the necessary equations for the more complex cases. This simple derivation can be found in any gas dynamics text, such as Ref. 24.

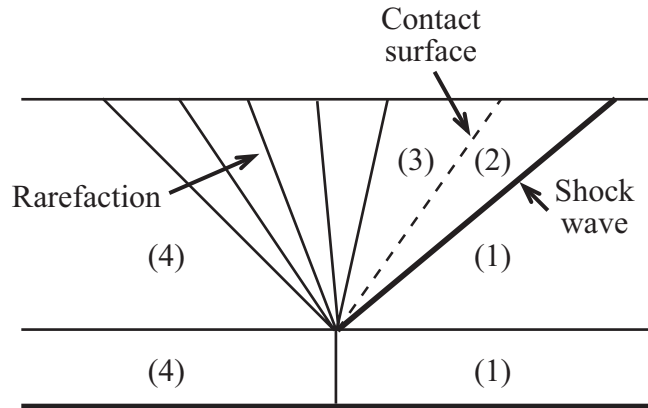


Fig. 4.1. Constant area shock tube.

Fig. 4.1 shows the evolution of the shock pattern created by the bursting of the diaphragm at time $t=t_0$. Prior to t_0 , the tube is separated into Region 4 and Region 1, with $P_4 \gg P_1$. The removal of the diaphragm generates a shock wave traveling through the low pressure region. The original barrier between the high and low pressure regions is maintained as the contact surface, which travels into the low pressure region behind the shock. Finally, a rarefaction propagates through the high pressure region. Depending on the initial pressure ratio, it may spread to both the right and left of the original diaphragm location or just to the left. Regions 2 and 3 consist of steady flow, which occur because the high pressure fluid can only be accelerated to a maximum "escape velocity," where all the potential energy of the quiescent fluid has been converted into kinetic energy. If the initial pressure ratio is not sufficiently high, regions of steady flow will not actually exist; the expansion will extend from the unperturbed Region 4 up to the contact surface. Nevertheless, the following analysis makes no assumptions about whether or not terminal velocity has been reached, and so will be valid regardless of the initial pressure ratio.

Pressures in Regions 1 and 4 are known, because they are unperturbed from the

initial conditions P_1 and P_4 , respectively. The Rankine-Hugoniot expressions provide a relationship between the velocity behind a shock and the pressure ratio across it.

$$u_2 = a_1 \left(\frac{P_2}{P_1} - 1 \right) \sqrt{\frac{2/\gamma}{(\gamma_1 + 1)P_2/P_1 + (\gamma_1 - 1)}} \quad (19)$$

Furthermore, assuming an isentropic expansion whose front is moving at the speed of sound in Region 4, an expression for the velocity in Region 3 is also available, via the isentropic relation:

$$u_3 = \frac{2a_4}{\gamma_4 - 1} \left[1 - \left(\frac{P_3}{P_4} \right)^{\frac{\gamma_4 - 1}{2\gamma_4}} \right] \quad (20)$$

By the definition of the contact surface, the pressures and velocities must be matched, therefore:

$$\begin{aligned} P_2 &= P_3 \\ u_2 &= u_3 = u_{\text{contact}} \end{aligned} \quad (21)$$

Setting Eq. (19) and Eq. (20) equal to each other yields an implicit relation for P_2/P_1 (which is equal to P_3/P_1).

$$\frac{P_4}{P_1} = \frac{P_2}{P_1} \left[1 - \frac{(\gamma_4 - 1)(a_1/a_4)(P_2/P_1 - 1)}{\sqrt{2\gamma_1(2\gamma_1 + (\gamma_1 + 1)(P_2/P_1 - 1))}} \right]^{\frac{-2\gamma_4}{\gamma_4 - 1}} \quad (22)$$

The result can be substituted back into Eq. (19) or Eq. (20) to find u_2 or u_3 .

4.3. Alpher and White's Method

It has been shown theoretically and experimentally that an area change near the diaphragm can be used to alter the strength of the resultant shock. Alpher and White¹ developed a quasi-steady, one-dimensional analysis for determining these strengths for the arbitrary diaphragm region geometry depicted in Fig. 4.2. This analysis is valid for a monotonic area change (solid line) or a convergence-divergence (dashed line). In the former case, A_{min} is equal to A_{small} .

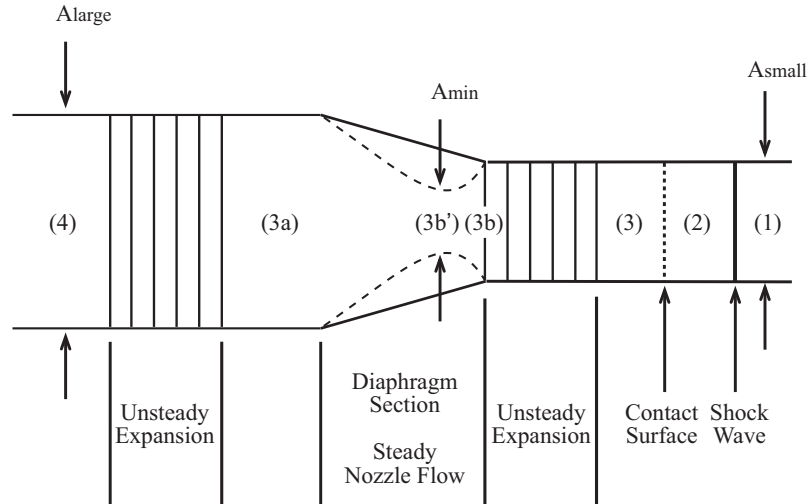


Fig. 4.2. Shock tube with area change at the diaphragm section.

It is assumed that within the area change section, there will be steady nozzle flow, with $M=1$ at the location of minimum cross-sectional area, A_{min} . Upstream of the area change, there will be an unsteady expansion connecting the nozzle to the unperturbed, high pressure region. Downstream of the nozzle, there will be another unsteady expansion, followed by a region of steady flow, analogous to Region 3 of the constant area shock tube. Next, there will be a contact surface, a second region of steady flow that

is analogous to Region 2 of the constant area tube, and a shock wave moving into the unperturbed low-pressure region.

One should note that the area change is assumed to be gradual enough that the flow through the area change remains isentropic. Referring to the original model shown in Fig. 2.1, this is a rather poor assumption. Since the entropy losses incurred by separation at an abrupt area change will serve to attenuate the strength of the rarefaction, and the motivation of this analysis is to prevent damage caused by the pressure drop, the gradual area assumption simply means that the estimate will be conservative.

It is also assumed that γ will remain constant in its respective fluid throughout this process. This may not necessarily be true for very large values of P_4/P_1 , especially if the gas is heated; however, incorporating the changes in γ has a negligible effect on the calculated pressure drop. γ may differ between the two fluids initially separated by the diaphragm.

In this model, the pressure drop in the larger area section will be $P_4 - P_{3a}$. It is more convenient to calculate the pressure drop as a non-dimensional quality, so pressure drop will be sought in the form $(1 - P_{3a}/P_4)$. As in the constant area tube, it is assumed that conditions in Regions 1 and 4 are known. The pressure ratio between the two regions can be expanded across all of the regions as follows:

$$\frac{P_4}{P_1} = \frac{P_4}{P_{3a}} \frac{P_{3a}}{P_{3b}} \frac{P_{3b}}{P_{3b'}} \frac{P_{3b'}}{P_3} \frac{P_3}{P_2} \frac{P_2}{P_1} \quad (23)$$

The first term, P_4/P_{3a} , will be the pressure ratio across an unsteady, centered expansion. This could also be seen as the pressure ratio necessary to accelerate the flow

from M_4 (which is 0) to M_{3a} . Assuming an isentropic process, the required pressure ratio is:

$$\frac{P_4}{P_{3a}} = \left(1 + \frac{\gamma_4 - 1}{2} M_{3a}^2 \right)^{\frac{2\gamma_4}{\gamma_4 - 1}} \quad (24)$$

The fourth term of the series, P_{3b}/P_3 is exactly the same condition, except that instead of accelerating the flow from 0 to M_{3a} , this pressure ratio must accelerate the flow from $M_{3b'}$ to M_3 . Therefore,

$$\frac{P_{3b}}{P_3} = \left(\frac{2 + (\gamma_4 - 1)M_{3b}^2}{2 + (\gamma_4 - 1)M_3^2} \right)^{\frac{2\gamma_4}{\gamma_4 - 1}} \quad (25)$$

In the area change section, the flow is expanded through a steady process, rather than an unsteady one. The second and third terms of Eq. (23) therefore become:

$$\frac{P_{3a}}{P_{3b'}} \frac{P_{3b'}}{P_{3b}} = \frac{P_{3a}}{P_{3b'}} = \left(\frac{2 + (\gamma_4 - 1)M_{3b}^2}{2 + (\gamma_4 - 1)M_{3a}^2} \right)^{\frac{\gamma_4}{\gamma_4 - 1}} \quad (26)$$

By the definition of contact surface, $P_3/P_2 = 1$. Substituting Eqs. (24), (25) and (26), Eq. (23) becomes:

$$\frac{P_4}{P_1} = \frac{P_2}{P_1} \left[\left(1 + \frac{\gamma_4 - 1}{2} M_{3a}^2 \right) \left(\frac{2 + (\gamma_4 - 1)M_{3b}^2}{2 + (\gamma_4 - 1)M_{3a}^2} \right)^{\frac{1}{2}} \left(\frac{2 + (\gamma_4 - 1)M_3^2}{2 + (\gamma_4 - 1)M_{3b}^2} \right) \right]^{\frac{2\gamma_4}{\gamma_4 - 1}} \quad (27)$$

For an ideal gas undergoing an isentropic process,

$$a(P)^{\frac{1-\gamma}{2\gamma}} = \text{const.} \quad (28)$$

Eq. (28) along with the pressure ratios expressed in Eqs. (24)-(26) can be used to construct a relationship between the Mach numbers in various parts of the tube.

$$M_3 = \frac{u_3}{a_3} = \frac{u_2 / a_1}{\frac{a_3}{a_{3b}} \frac{a_{3b}}{a_{3a}} \frac{a_{3a}}{a_4} \frac{a_4}{a_1}} \quad (29)$$

$$= \left[\left(\frac{a_1}{u_2} \frac{a_4}{a_1} \sqrt{\frac{2 + (\gamma_4 - 1)M_{3a}^2}{2 + (\gamma_4 - 1)M_{3b}^2}} \frac{2 + (\gamma_4 - 1)M_{3b}}{2 + (\gamma_4 - 1)M_{3a}} \right) - \frac{\gamma_4 - 1}{2} \right]^{-1}$$

Finally, by assuming steady flow in the nozzle, area and Mach number can be related by combining the isentropic equation with conservation of mass.

$$\frac{A_{large}}{A_{small}} = \frac{M_{3b}}{M_{3a}} \left(\frac{2 + (\gamma_4 - 1)M_{3a}^2}{2 + (\gamma_4 - 1)M_{3b}^2} \right)^{\frac{\gamma_4 + 1}{2(\gamma_4 - 1)}} \quad (30)$$

The shock wave and contact surface are just as in the constant area case, so Eq. (19) and (21) remain valid. Collecting Eqs. (19), (27), (29) and (30) gives a system of four equations for five unknowns: M_3 , M_{3a} , M_{3b} , p_2/p_1 and u_2/a_1 . The fifth equation necessary to solve the system will depend on whether the flow is sub- or supersonic. If the flow is subsonic, the expansion separating Region 3 and Region 3b will not exist. Therefore,

$$\begin{aligned}
M_3 &= M_{3b} \\
P_3 &= P_{3b} \\
a_3 &= a_{3b}
\end{aligned}
\tag{31}$$

If the flow is supersonic, choking will occur at the minimum area section, so $M_{3b}=1$. Similar to Eq. (30), the Mach number in Region 3a can be related to the Mach number in Region 3b' as a function of the area ratio.

$$\frac{A_{min}}{A_{small}} = M_{3b} \left[\frac{1 + \gamma_4}{2 + (\gamma_4 - 1)M_{3b}^2} \right]^{\frac{\gamma_4 + 1}{2(\gamma_4 - 1)}}
\tag{32}$$

If the area change is monotonic, Eq. (32) is unnecessary, because A_1 will be the minimum area, so $M_{3b}=1$, which can be substituted directly into Eqs. (27), (29) and (30). In this case, note that M_{3b} is a function *only* of the area ratio. Furthermore, from Eq. (30), M_{3a} will also only be a function of area ratio. M_3 , however, is also a function of the initial pressure ratio. Therefore, the flow speed, and thus the pressure drop in the larger diameter portion of the tube can be limited by an appropriately designed area change section while still permitting a range of shock strengths.

Because of this fact, it is not actually necessary to know, *a priori*, whether the flow will be sub- or supersonic. Instead, the minimum initial pressure ratio necessary to choke the flow, $(P_4/P_1)_{min}$ can be found by using the subsonic analysis and assuming that $M_{3b}=1$. This is valid, because at the smallest possible pressure ratio that will produce sonic flow, there will still be no expansion between Regions 3b and 3. This will produce a system of six equations, and six unknowns (the additional one being $(P_4/P_1)_{min}$). If

(P_4/P_1) is greater than $(P_4/P_1)_{min}$, then the flow is supersonic; if it is less, it will be subsonic.

When Alpher and White performed their analysis, few computational tools were available. The authors defined and plotted a number of intermediary functions which have no obvious physical significance. These plots could be used in series to determine the necessary diaphragm pressure ratio to achieve a desired Mach number. Today, using a mathematical software package such as Maple, Matlab or Mathematica, the system can readily be solved directly, making this method much more practical than it was when the method was originally derived.

4.4. Igra and Gottlieb's Method for Area Expansions

Igra and Gottlieb¹⁶ used a similar method to model the pattern of flow established as a rarefaction propagates through an area enlargement. As the rarefaction is reflected, it will condense into a compression wave, and possibly a shock. The idea of Igra and Gottlieb's method is to ignore the transient condensation process, and assume that the transmitted and reflected waves will eventually reach a steady strength. This pattern is shown in Fig. 4.3. Recall that since flow moves from left to right, expansion propagation is from right to left. The incoming rarefaction has a pressure ratio of P_2/P_1 . The transmitted portion of the rarefaction will have a pressure ratio of P_3/P_1 . This is the quantity of interest, since it represents the pressure drop conveyed to the pressure vessel. The remainder of the rarefaction is reflected as a compression wave of strength P_3/P_2 , i. e., a shock. Accelerating the flow out of the area change will be a third rarefaction wave of strength P_3/P_4 . This shall be designated Pattern B. If the incident reflection is not strong enough to generate supersonic flow in the smaller pipe, the rarefaction will not be

present, i.e.: conditions in (4) are equal to those in (3). Furthermore, the shock will actually only be a compression, although the Rankine-Hugoniot equations (which are still valid for very weak shocks) will still be used to calculate the pressure drop. This shall be designated Pattern A. The methods for analyzing both patterns are nearly identical.

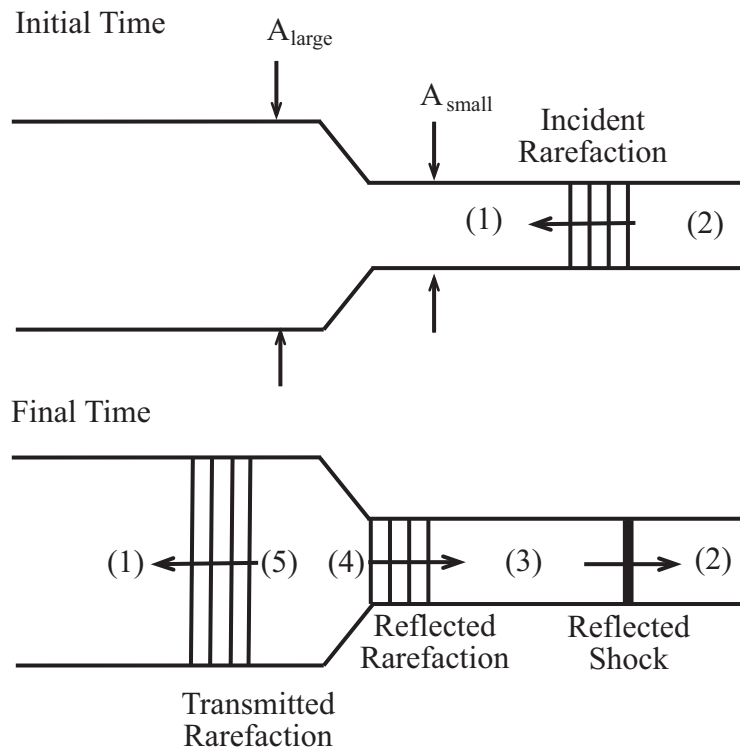


Fig. 4.3. Flow pattern as a rarefaction encounters an increase in area.

It should be noted that this analysis treats a rarefaction as it moves into the left, high pressure portion of the shock tube. The low pressure gas is not present at all in these calculations. Therefore, the subscripts on γ shall be dropped, but the reader should be aware that it corresponds to the specific heat ratio of the high pressure gas, which is once again assumed to be constant. In a case where there were initially different gases on

either side of the area discontinuity, the subscripts would need to be retained.

Furthermore, a contact surface would be present between the downstream propagating shock and rarefaction, separating the two gases. This contact surface is shown in Igra and Gottlieb's¹⁶ paper, but is omitted here for simplicity.

As in Eq. (19), the Rankine-Hugoniot equations shall be used to relate the properties in Region 2 to those in Region 3.

$$u_3 = u_2 - a_2 \left(\frac{P_3}{P_2} - 1 \right) \sqrt{\frac{2/\gamma}{(\gamma_1 + 1)P_3/P_2 + (\gamma_1 - 1)}} \quad (33)$$

$$a_3 = a_2 \sqrt{\frac{\frac{P_3}{P_2} \frac{\gamma + 1}{\gamma - 1} + \frac{P_3}{P_2}}{1 + \frac{P_3}{P_2} \frac{\gamma + 1}{\gamma - 1}}} \quad (34)$$

All expansions are assumed to be isentropic, so

$$\frac{P_2}{P_1}^{\frac{\gamma-1}{2\gamma}} = \frac{a_2}{a_1} \quad (35)$$

Finally, creating a characteristic line connecting Regions 1 and 2 yields:

$$\frac{2}{\gamma-1} a_2 - u_2 = \frac{2}{\gamma-1} a_1 - u_1 = \frac{2}{\gamma-1} a_1 \quad (36)$$

Assuming that the conditions in Regions (1) and (2) are known (i.e., given an input rarefaction), Eqs. (33)-(36) can be used to solve for P_3 , a_3 and u_3 .

As in Alpher and White's analysis, flow through the area change is assumed to be isentropic. Conserving mass flow and energy in a manner similar to Eq. (30),

$$\begin{aligned} \frac{P_4}{P_5} &= \left(\frac{T_4}{T_5} \right)^{\frac{\gamma}{\gamma-1}} = \left(\frac{a_4}{a_5} \right)^{\frac{2\gamma}{\gamma-1}} \\ &= \left(\frac{\rho_4}{\rho_5} \right)^{\gamma} = \left(\frac{M_5}{M_4} \frac{A_{large}}{A_{small}} \right)^{\frac{2\gamma}{\gamma+1}} = \left(\frac{2 + (\gamma-1)M_5^2}{2 + (\gamma-1)M_4^2} \right)^{\frac{\gamma}{\gamma-1}} \end{aligned} \quad (37)$$

If Pattern B exists, the flow downstream of the area change must be supersonic, meaning that $M_4=1$. Since the area relation is known, Eq. (37) can be used to solve for M_5 directly. If the flow is subsonic, $P_3 = P_4$ and $u_3 = u_4$. Since reflection process is assumed to be isentropic,

$$\frac{P_4}{P_1} = \left(\frac{a_4}{a_1} \right)^{\frac{2\gamma}{\gamma-1}} \quad (38)$$

$M_4=u_4/a_4$ can be used to solve Eq. (37) for M_5 . Finally, as in Eq. (36), a characteristic can connect Regions 1 and 5. The velocity in Region 1 is zero because it is unperturbed.

$$\frac{2}{\gamma-1} a_5 - u_5 = a_5 \left(\frac{2}{\gamma-1} - M_5 \right) = \frac{2}{\gamma-1} a_1 - u_1 = \frac{2}{\gamma-1} a_1 \quad (39)$$

The isentropic relation then yields the transmitted rarefaction pressure ratio,

$$\frac{P_5}{P_1} = \left(\frac{a_5}{a_1} \right)^{\frac{2\gamma}{\gamma-1}} \quad (40)$$

The only remaining problem is how to determine whether the flow will take the form of Pattern A or Pattern B. This is done by calculating the minimum pressure ratio $(P_2/P_1)_{min}$ necessary to generate Mach 1 in Region 4. As in the Alpher-White analysis, a further increase in this pressure ratio will have no effect on the transmitted rarefaction, due to the choking. $(P_2/P_1)_{min}$ cannot be solved for directly, but because the resulting minimum transmission pressure ratio, $(P_5/P_1)_{min}$ corresponds to $M_4=1$, it can be solved using Eqs. (37),(39) and (40). Given $(P_5/P_1)_{min}$, the procedure for Pattern B is worked backward, resulting in $(P_2/P_1)_{min}$. If the input pressure ratio is greater than $(P_2/P_1)_{min}$, then P_5/P_1 will equal $(P_5/P_1)_{min}$. If it is less than $(P_2/P_1)_{min}$ then the problem must be solved assuming Pattern A.

4.5. Gottlieb and Igra's Method for Area Contractions

Gottlieb and Igra actually studied the flow patterns through an area contraction before their work on area enlargements, but as the latter case was a logical continuation from Alpher and White's Method, it was presented first. The main complication of treating a contraction instead of a rarefaction is that there are four possible steady-state wave patterns instead of two, one subsonic and three supersonic, labeled A-D. Each contains between five and seven regions of steady flow.

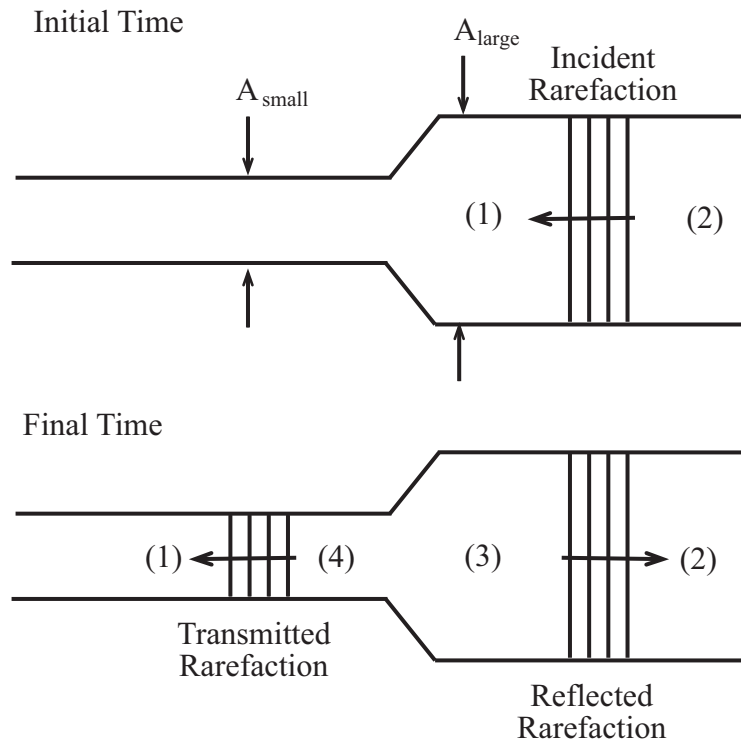


Fig. 4.4. Subsonic flow pattern as a rarefaction encounters an increase in area.

In a general case of an area contraction upstream of the orifice, where the contracted area is greater than the effective orifice area, the case simplifies, since the flow is guaranteed to be subsonic. Pattern A, the subsonic case, shown in Figure Fig. 4.4, consists of the simplest system possible: one incident rarefaction, one reflected rarefaction, and one transmitted rarefaction. This is very similar to the acoustic case studied earlier, where the waves are defined as nonlinear rarefactions, rather than unit steps. This yields a simple system of equations, familiar to the area expansion case.

Regions 1 and 4 and 1 and 2 are each connected by a negative characteristic.

$$\frac{2a_4}{\gamma-1} - u_4 = \frac{2a_1}{\gamma-1} - u_1 \Rightarrow \frac{a_4}{a_1} \frac{2}{\gamma-1} - \frac{u_4}{a_4} = \frac{2}{\gamma-1} \quad (41)$$

$$\frac{a_2}{a_1} \frac{2}{\gamma-1} - \frac{u_2}{a_2} = \frac{2}{\gamma-1} \quad (42)$$

Regions 2 and 3 are connected by a positive characteristic.

$$\frac{a_3}{a_1} \frac{2}{\gamma-1} + \frac{u_3}{a_1} = \frac{a_2}{a_1} \frac{2}{\gamma-1} + \frac{u_2}{a_1} \quad (43)$$

As in Eq. (37) flow through an isentropic area change yields

$$\left(\frac{u_4}{a_4} \frac{a_3}{u_3} \frac{A_{small}}{A_{big}} \right)^{\frac{2\gamma}{\gamma+1}} = \left(\frac{a_3}{a_4} \right)^{\frac{2\gamma}{\gamma-1}} = \left(\frac{2 + \frac{(\gamma-1)u_4^2}{a_4^2}}{2 + \frac{(\gamma-1)u_3^2}{a_3^2}} \right)^{\frac{\gamma}{\gamma-1}} \quad (44)$$

a_2/a_1 can be found explicitly from the isentropic relation, since P_2/P_1 is given.

u_2/u_1 can then be found from Eq. (42). This is a system of four equations for four unknowns: u_4/a_1 , u_3/a_1 , a_4/a_1 , and a_3/a_1 . P_4/P_1 and P_3/P_1 can then be found using the isentropic relationship on the speed of sound ratios. The value of P_4/P_1 should be greater than the minimum transmitted pressure ratio, $[2\gamma/(\gamma+1)]^{\frac{2\gamma}{\gamma-1}}$, otherwise, the flow is not fully subsonic, and Pattern A is incorrect.

If the diaphragm is close to the orifice, Alpher and White's method is very convenient for analyzing a number of area changes lumped as one in the steady nozzle flow region. This is especially opportune since the fittings of the orifice may result in a complicated geometry in that section of the tunnel. Nevertheless, if the diaphragm is far

downstream of the orifice, Alpher and White's technique may not be applicable, and one of the three supersonic patterns must be invoked. In Alpher and White's method, the disturbance is generated within the area change section, and there is only one possible supersonic downstream flow configuration. In Gottlieb and Igra's method, the disturbance is generated somewhere downstream, which allows for three possible supersonic patterns based on the value of z and the magnitude of the area change. Both methods generate the same upstream conditions, because they treat the choking condition in an identical manner. The differences in the results between the two methods bring up interesting questions, but for the purpose of this research, the differences are irrelevant. The area of interest is *upstream* of the orifice. As long as the orifice is choked, flow conditions downstream cannot have any bearing on the conditions in the heater. As such, there is no difference in the two treatments, and the remainder of Gottlieb and Igra's method shall not be discussed. If the reader is interested in conditions upstream of the orifice, Reference 13 contains more details on the derivation of Patterns B-D, as well as the flow regimes where each is applicable.

4.6. Application to the Problem

In the present work, the methods described above have been used in sequence in order to evaluate a complex geometry, such as the model tunnel shown in Fig. 2.1. The transition from A_1 through the constriction of the orifice to A_2 is modeled using Alpher and White's method for a converging-diverging nozzle. If one wished to examine the case of no metering orifice the monotonically-converging version of this method would be more appropriate. Either method will generate a pressure ratio for the transmitted rarefaction, P_{3a}/P_4 , as defined in Fig. 4.2.

At the pipe bend, in order for the junction to be properly mitered, the cross-sectional area of the angled pipe will be less than the horizontal pipe. The transmitted pressure ratio generated by Alpher and White's procedure then becomes the input pressure ratio for Gottlieb and Igra's method for area reductions. A_{big} and A_{small} in Fig. 4.3 will become A_2 and A_3 from Fig. 2.1, respectively. This will generate a transmitted and reflected pressure drop. Here it should be noted that the area of the angled pipe must be larger than the effective orifice area, otherwise the flow would choke at the pipe bend, rather than the orifice. This could have very dangerous results for the tunnel, namely a standing shock in the angled pipe and a Prandtl-Meyer corner expansion at the junction with the horizontal pipe. One of the supersonic patterns discussed in Section 4.5 could be used to calculate the pressure drop, but it could not take into account the two-dimensional effects caused by the expansion fan. For the purposes of this work, it will be assumed that the tunnel has been properly designed to choke at the orifice, but one should take caution when applying these results to a generic scenario where choking may not be guaranteed.

The next area junction in the model tunnel is a three-pipe junction, for which there is no assumed flow pattern. Nevertheless, it can be shown that, as in the acoustic method, a junction of n pipes can be modeled as an area enlargement, where

$$A_{big} = \sum_{n=1..i} A_i .$$

The transmitted pressure ratio generated by Gottlieb and Igra's area

contraction procedure then becomes the input pressure ratio for their area expansion method. In this case, A_{small} and A_{large} of Fig. 4.3 will become A_3 and $2A_4$ from Fig. 2.1, respectively. These inputs are sufficient to generate the pressure ratio transmitted into the pressure vessel, (P_6/P_1 in Fig. 4.3) as well as the compression ratio of the reflected shock (P_2/P_3 in Fig. 4.3). This transmitted pressure ratio can be used as an input pressure ratio

for a second Igra and Gottlieb analysis as the rarefaction moves through the area change into the bottom half of pressure vessel, exactly as before.

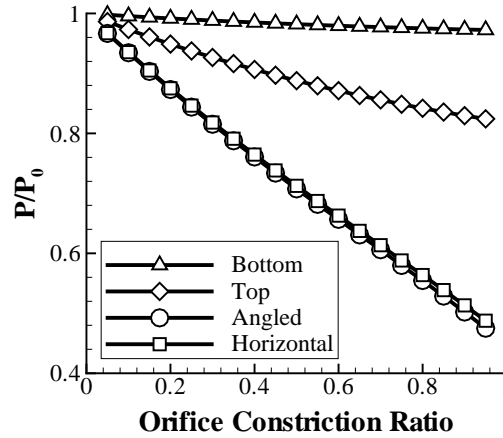


Fig. 4.5. Results of flow pattern assumption methods.

The above procedures demonstrate the way the pressure peaks and valleys can be predicted for a system of a given geometry. Each of the methods have been previously derived by other authors, but this is the first work in which they have been combined in sequence to analyze a network of pipes, rather than a single area discontinuity in isolation. Fig. 4.5 shows the predicted pressures in the horizontal pipe, the angled pipe, and in the upper and lower sections of the heater as a function of C . The flow pattern method predicts identical pressure drops in the top and middle of the heater. Although this model includes only three area changes after the orifice, Igra and Gottlieb's methods for area contractions and expansions could be iterated any number of times. Not shown are the reflections off the top and bottom of the heater. None of these methods account for reflections from solid boundaries, and, indeed, the region is non-simple, since it involves the interaction of two rarefaction waves. For simplicity, the acoustic

approximation can be used, and the pressure drop can be assumed to be doubled at the solid boundary.

One interesting result of this analysis is that the transmitted pressure drop is a function of only one variable, but whether the chosen variable is C or z depends on whether the flow is sub- or supersonic, determined by whether or not a minimum initial pressure ratio is exceeded. This minimum pressure ratio is set by the orifice size. If the incident pressure ratio is below that threshold value, the result will be subsonic flow. Without choking, the presence of the orifice will be irrelevant and the transmitted pressure drop will be a function of initial pressure ratio only. If the initial pressure ratio is high enough that the flow is supersonic, the transmitted pressure ratio will not depend on incident pressure ratio, only on orifice area. Since this investigation is geared toward hypersonic tunnels, this means that the pressure drop will depend only on the effective area of the orifice. On one hand, this means that the orifice is not as effective in metering the flow as it would be for a subsonic flow. However, it also means that since transmitted pressure ratio is not a function of incident pressure ratio, a single orifice design should be sufficient to protect the heater in any run conditions.

It would seem as though an obvious solution would be to put in a very small metering orifice to damp out the majority of the rarefaction. However, once steady flow is established, if the metering orifice is a smaller diameter than the throat of the actual tunnel nozzle, it will prevent adequate mass flow from reaching the test section. Therefore, it is critical that the minimum possible effective area for the metering orifice is still larger than the throat. If that does not give sufficient pressure drop protection, a variable-area valve or ablative orifice may be used.

As a final cautionary note, in a later analysis, Igra, Wang and Falcovitz found that supersonic flow through an area contraction was dominated by two-dimension effects, and this quasi-steady method was a poor predictor of performance¹⁷. For the majority of the area changes considered in this paper, the flow is subsonic, so there will be none of the corner expansions or oblique shocks that were observed by Igra, Wang and Falcovitz. The only area that might be affected would be directly downstream of the orifice, an area which is mostly neglected in this work, but which could be of potential interest in a different study.

5. The Method of Characteristics

5.1. Description of the Method

The Method of Characteristics is a general solution method for any hyperbolic partial differential equation combined with a set of known conditions. In a two-dimensional, steady application, those conditions would be imposed along a one-dimensional line in space in the upstream portion of the computational region. For a one-dimensional, unsteady problem, they would be the initial conditions over the spatial domain. The Method of Characteristics essentially locates specific spatial or spatial-temporal lines, called characteristics, along which the governing PDEs simplify to ODEs, or in some special cases, algebraic expressions.

Unlike the previously described methods, which contain certain assumptions in their derivations, the user must choose which assumptions to include when utilizing the Method of Characteristics. It will be seen that some assumptions will result in huge simplifications to the method. Here, the following assumptions shall be made, as in Kentfield²²:

- Flow is one-dimensional (channel area varies only as a function of x).
- Flow is unsteady.
- Flow is compressible.
- Wall friction is accounted for through a frictional force.
- Ratio of specific heats, γ , is constant.

Unlike Kentfield, heat transfer to and from the duct walls and the thermal influences of chemical reactions shall be neglected, as they are of negligible significance

to the application of interest. Comparing these assumptions to those contained in the first two methods, it can be seen that the Method of Characteristics has two main advantages: unsteady effects and frictional forces can now be considered, through the use of finite differences. As before, changes in γ are believed to be negligible in this flow. The only inappropriate assumption, therefore, is that of one-dimensional flow. However, since the Method of Characteristics will already reveal the effects of unsteady and frictional flow, it is best to present a one-dimensional version, which would distinguish the effects of these differences, and *then* perform an axisymmetric analysis, providing further information on the effects of two dimensional flow. In fact, although the governing equations shall be derived by including entropy terms, only the isentropic results have been computed. This will demonstrate the effects of unsteadiness over the earlier, steady methods. A second program could be written with entropy terms (including friction and separation at area junctions) to demonstrate the effect of entropy losses, but that is beyond the scope of the present work, as is the other logical step in the progression, a two-dimensional, unsteady analysis.

5.2. Derivation of Governing Equations

In order to implement the Method of Characteristics, the governing partial differential equations must be first be determined. In this case, the governing equation is actually a set of three equations, representing continuity of mass, momentum and energy. The following notation is used for the substantial derivative in one dimension:

$$S \equiv \frac{D}{Dt} = \frac{\partial(\)}{\partial t} + u \frac{\partial}{\partial x}(\) \quad (45)$$

Conservation of mass:

$$S\rho + \rho \frac{\partial u}{\partial x} + \frac{\rho u}{A} \frac{dA}{dx} = 0 \quad (46)$$

Conservation of momentum:

$$Su + \frac{1}{\rho} \frac{\partial P}{\partial x} + f = 0 \quad (47)$$

Conservation of energy:

$$Sh - \frac{1}{\rho} SP - uf = 0 \quad (48)$$

where f is defined as the frictional wall force per unit mass of fluid, and h is the enthalpy.

Using the ideal gas law, the first law of thermodynamics and the definitions of speed of sound and enthalpy, the following differential relations can be obtained:

$$\frac{d\rho}{\rho} = \frac{2}{\gamma-1} \frac{da}{a} - \frac{ds}{R} \quad (49)$$

$$\frac{dP}{P} = \frac{2\gamma}{\gamma-1} \frac{da}{a} - \frac{ds}{R} \quad (50)$$

$$dh - \frac{dP}{\rho} = c_p dT - \frac{dP}{\rho} = \frac{1}{\gamma} \frac{a^2}{R} ds \quad (51)$$

These relations can be substituted into Eqs. (46)-(48) to replace P , ρ and h with a and s .

$$Sa + a \frac{\partial}{\partial x} \left(\frac{\gamma-1}{2} u \right) = \left(\frac{\gamma-1}{2} \right) \left[\frac{\rho f}{a} - a \frac{u}{A} \frac{dA}{dx} \right] \quad (52)$$

$$S \left(\frac{\gamma-1}{2} u \right) + a \frac{\partial a}{\partial x} = \frac{a^2}{2c_p} \frac{\partial s}{\partial x} - \left(\frac{\gamma-1}{2} \right) f \quad (53)$$

$$Ss = \frac{\gamma R}{a^2} u f \quad (54)$$

At this point, the substantial derivative will be replaced with two new differential operators, M and N .

$$\begin{aligned} M &\equiv S - a \frac{\partial(\quad)}{\partial x} = \frac{\partial(\quad)}{\partial t} + (u-a) \frac{\partial(\quad)}{\partial x} \\ N &\equiv S + a \frac{\partial(\quad)}{\partial x} = \frac{\partial(\quad)}{\partial t} + (u+a) \frac{\partial(\quad)}{\partial x} \end{aligned} \quad (55)$$

M and N can be thought of as the variation of some variable along lines of slope $1/(u-a)$ or $1/(u+a)$, respectively, in the way that the substantial derivative is the change of some variable along a line of slope $1/u$. Specifically, M and N will act upon two variables, m and n , known as the Riemann invariants.

$$\begin{aligned}
m &\equiv a - \frac{\gamma - 1}{2} u \\
n &\equiv a + \frac{\gamma - 1}{2} u
\end{aligned}
\tag{56}$$

Rewriting Eqs. (52)-(54) again,

$$Mm = \frac{\gamma - 1}{2} \left[\frac{\gamma}{a} uf - a \frac{u}{A} \frac{dA}{dx} \right] - \frac{a^2}{2c_p} \frac{\partial s}{\partial x} + \frac{\gamma - 1}{2} f
\tag{57}$$

$$Nn = \frac{\gamma - 1}{2} \left[\frac{\gamma}{a} uf - a \frac{u}{A} \frac{dA}{dx} \right] + \frac{a^2}{2c_p} \frac{\partial s}{\partial x} - \frac{\gamma - 1}{2} f
\tag{58}$$

$$Ss = \frac{\gamma R}{a^2} uf
\tag{59}$$

One immediately obvious result is that if the flow is homotropic (i.e., isentropic everywhere) and happens to be in a constant area pipe, Eq's (57) and (58) reduce to

$$\begin{aligned}
Mm &= 0 \\
Nn &= 0
\end{aligned}
\tag{60}$$

and Eq. (59) becomes extraneous. Therefore, m is constant along lines with slope $1/(u-a)$, and n is constant along lines with slope $1/(u+a)$. This will provide an exact solution to the partial differential equation. If the solution is not homotropic, Eqs. (57)-(59) can be solved using a finite difference routine. Assuming $u < 0$ (as it is in the model problem), for stability, m should be found using forward differencing, and n using backward differencing in subsonic flow, and forward differencing in supersonic flow³¹.

Furthermore, it can be convenient to nondimensionalize the equations, so from this point forward, Eqs. (57)-(59) will be replaced with:

$$M'm' = \frac{\gamma-1}{2} \left[\frac{u'f'}{a'} - a'u' \frac{dA'}{dx'} \right] - \frac{\gamma-1}{2\gamma} a'^2 \frac{\partial s}{\partial x} + \frac{\gamma-1}{2\gamma} f' \quad (61)$$

$$N'n' = \frac{\gamma-1}{2} \left[\frac{u'f'}{a'} - a'u' \frac{dA'}{dx'} \right] + \frac{\gamma-1}{2\gamma} a'^2 \frac{\partial s}{\partial x} - \frac{\gamma-1}{2\gamma} f' \quad (62)$$

$$S's' = \frac{u'f'}{a'^2} \quad (63)$$

using

$$\begin{aligned} dA' &\equiv \frac{dA}{A} \\ \frac{dA'}{dx'} &\equiv \frac{L_{ref}}{A} \frac{dA}{dx} \\ a' &\equiv a / a_{ref} \\ f' &\equiv \gamma f L_{ref} / a_{ref}^2 \\ m' &\equiv m / a_{ref} \\ n' &\equiv n / a_{ref} \\ s' &\equiv s / R \\ t' &\equiv t a_{ref} / L_{ref} \\ x' &\equiv x / L_{ref} \\ u' &\equiv u / a_{ref} \\ P' &\equiv P / P_{ref} \\ M' &\equiv (L_{ref} / a_{ref}) M \\ N' &\equiv (L_{ref} / a_{ref}) N \\ S' &\equiv (L_{ref} / a_{ref}) S \end{aligned} \quad (64)$$

where a_{ref} and L_{ref} are reference speed of sound and length, respectively. There is an implicit s_{ref} as well, which is assumed to be 0.

If initial conditions are known, conditions at a timestep $\Delta t'$ in the future, n' , m' and s' at a point x' can be found by tracing the appropriate characteristics back to the initial conditions. If the flow is not homotropic (i.e., m' and n' are not constant along their respective characteristics) finite differences can be used to find the new invariants. Then velocity and speed of sound can be found by rearranging Eq. (56):

$$\begin{aligned} a' &= \frac{m'+n'}{2} \\ u' &= \frac{n'-m'}{\gamma-1} \end{aligned} \quad (65)$$

From Eq. (50) it can be shown that

$$P' = e^{-s'} (a')^{\frac{2\gamma}{\gamma-1}} \quad (66)$$

Conditions at $t'=2\Delta t'$ can then be determined by tracing characteristics back to the conditions at $t'=\Delta t'$ and so on until the desired time has been reached.

5.3. Application to the Problem

5.3.1. Set-Up

As in the analysis of transient pipe pressures, the Method of Characteristics will be applied to an array of N constant-area pipes (pipe areas can differ between pipes, but are constant along a given pipe), each of which contains J(N)-1 internal nodes. The pipes

will be labeled in the direction of rarefaction travel; therefore Pipe 1 will be the pipe which is furthest downstream.

Initial conditions are assigned to each node. Reference values will be taken as pressurized tank conditions. Therefore, for points upstream of the diaphragm, $P'=a'=1$ and $u'=0$. Downstream of the diaphragm, $P'=P_{low}/P_{high}$, $a'=\left(P_{high}/P_{low}\right)^{\frac{\gamma-1}{2\gamma}}$ and $u'=0$. Since a' and u' are known, values of m' and n' can be found using Eq. (56).

5.3.2. Internal Points

Because the slopes of the characteristic lines are dependent variables, there is no guarantee that they will pass through any computational grid points aside from the initial line of data. Although schemes exist which can take data from several spatial points away, this can cause severe problems at the boundaries. Instead, the $\Delta t'$ and $\Delta x'$ are chosen such that the slope any given characteristic line is less than $\Delta t'/\Delta x'$, meaning that conditions at point (x',t') , $0 < x' < 1$ (assuming the l_{ref} is the length of the pipe) can be always found given conditions at $(x'-\Delta x', t'-\Delta t')$, $(x', t'-\Delta t')$ and $(x'+\Delta x', t'-\Delta t')$. This gives the CFL condition for stability⁴¹:

$$\Delta t' \leq \frac{\Delta x'}{|u'_{\max}| + |a'_{\max}|} \quad (67)$$

Here, a variable $\Delta t'$ will be used, where $\Delta t'$ is reset at each time step, based on the maximum values of u' and a' at the current time. If the flow is not homotropic, $\Delta t'$ should be multiplied by a safety factor, since the CFL condition is really only valid for linear partial differential equations³.

Next, values at (x', t') are determined by interpolating the Riemann invariants from either $(x', t' - \Delta t')$ and $(x' - \Delta x', t' - \Delta t')$ or $(x', t' - \Delta t')$ and $(x' + \Delta x', t' - \Delta t')$ depending on the sign of the slope of the characteristic. Consider an M' characteristic with slope β'_m at (x, t) .

$$\beta'_m(x', t') = \frac{\Delta t'}{\Delta x'} [u'(x', t' - \Delta t') - a'(x', t' - \Delta t')] \quad (68)$$

If β'_m is positive, m' will be found from points $(x', t' - \Delta t')$ and $(x' - \Delta x', t' - \Delta t')$.

$$m'(x', t') = \beta'_m m'(x' - \Delta x', t' - \Delta t') + (1 - \beta'_m) m'(x', t' - \Delta t') + M' m' \quad (69)$$

If β'_m is negative, m' will be found from points $(x', t' - \Delta t')$ and $(x' + \Delta x', t' - \Delta t')$.

$$m'(x', t') = |\beta'_m| m'(x' + \Delta x', t' - \Delta t') + (1 - |\beta'_m|) m'(x', t' - \Delta t') + M' m' \quad (70)$$

For an N' characteristic,

$$\beta'_n(x', t') = \frac{\Delta t'}{\Delta x'} [u'(x', t' - \Delta t') + a'(x', t' - \Delta t')] \quad (71)$$

n' can then be found by using Eqs. (69) or (70) as appropriate with every m' replaced with an n' and every β'_m with a β'_n . If the flow is not homotropic, s' must also be considered.

$$\beta'_s = \frac{\Delta t'}{\Delta x'} u'(x', t' - \Delta t') \quad (72)$$

Again, Eqs. (69) and (70) can be used, this time with s' .

The only remaining difficulty is the $M'm'$, $N'n'$ and $S's'$ terms. In homotropic flow, they will go to zero. Furthermore, $s' \equiv 0$, so the S' characteristics can be left out of the

problem altogether. However, if the flow is not homotropic, one can substitute Eqs (61), (62) or (63) into (69) or (70) as appropriate. Changing the differential to a difference, the values of q' , u' , a' , f' , and dA'/dx' can be interpolated along the characteristic from the previous time step, in the same manner as m' and n' . In many cases, q' , f' and dA'/dx' will constant with time.

Once m' and n' are known, a' , u' and P' can be found from Equations (65) and (66).

5.3.3. Boundaries

If a point lies on the boundary of the computational region, either $(x'-\Delta x', t')$ or $(x'+\Delta x', t')$ will be available, but not both. If the flow is subsonic (but not zero velocity) either m' or n' will be known, but not both. s' may or may not be known, depending on the direction of the flow. If the flow is supersonic, all the characteristics will be swept in the direction of the flow, so either all three will be known, or none will. From what we know of the problem already, the flow will be subsonic upstream of the orifice, sonic in the orifice, and supersonic downstream of the orifice. First, the subsonic boundary conditions will be considered, followed by flow through a choked orifice, and finally, supersonic outflow. In this section, the notation will change slightly to include the pipe number. Therefore, pressure at x and t of Pipe i shall be denoted $P(i,x,t)$. Since there are N interior points to each pipe (where N can be a function of i) the upstream boundary of each pipe will be at $x=\Delta x (N+1)$ and the downstream boundary at $x=0$.

5.3.3.1. Closed End

As part of the no-slip boundary, the flow velocity u' at a solid, stationary boundary is zero. From Eq. (65) the cases for a closed downstream or upstream end are, respectively

$$\begin{aligned} n'(i,0,t) &= m'(i,0,t) \\ m'(i,\Delta x(N+1),t) &= n'(i,\Delta x(N+1),t) \end{aligned} \quad (73)$$

From Eq. (72), for either case,

$$\beta'_s = 0 \quad (74)$$

5.3.3.2. Multi-Pipe Junction

For a multi-pipe junction, the basic conditions which must be met are the same as for the acoustic case, where continuity of pressure and velocity must be enforced. It is assumed that no significant volume is enclosed at the actual pipe junction (i.e., no plenum).

For homotropic flow, a simple algorithm is given by Kentfield²² for a junction of n pipes provides conditions in pipe r .

$$\lambda_{unknown,r} = \sum_{i=1}^n (K_i \lambda_{known,i}) - \lambda_{known,r} \quad (75)$$

where

$$K_i \equiv \frac{2A_i}{A_{total}} \quad (76)$$

and

$$A_{total} = \sum_{i=1}^n A_i \quad (77)$$

$\lambda_{unknown,r}$ is whichever of m' or n' is unknown at the boundary of pipe r and $\lambda_{known,r}$ is the one which is known. Since the flow is assumed to be homotropic, $s'=0$.

If one wishes to consider more realistic flow through an area change, the boundary condition becomes decidedly more complex, due to separation and the presence of a *vena contracta*. One would likely need to incorporate loss coefficients, which are highly dependent on the precise geometry of the area change. Alternately, instead of treating an area discontinuity as a boundary, one could treat the area change via the dA/dx term of Equation (52). This method is described at length Section IV.g of Ref. 37. Both methods are beyond the scope of the paper, and only the homotropic case will be considered.

5.3.3.3. Choke Point

If the flow through an orifice is subsonic, conditions can be found by using the area discontinuity method described in the previous section. However, much like the acoustic method, this boundary condition contains no choking limit, so one must be artificially introduced. Although Kentfield presents some criteria for determining whether inflow and outflow will be sub- or supercritical, these criteria assume there is an imposed inlet or outlet pressure. Although one could replace this imposed pressure with the pressure from the adjoining pipe, this can, in practice, lead to oscillatory behavior in a numerical implementation. The author has found that it is easier to calculate the subcritical case, and if it produces a result where the Mach number is greater than one, to replace it with the choked case.

Assume the orifice is Pipe i , with the upstream pipe being Pipe $i+1$ and the downstream pipe being $i-1$. The downstream pipe will be dealt with first. From Equation (65), we can see in order to force $u=-a$ (recall that the problem is set up such that flow downstream is negative),

$$m'(i,0,t) = \frac{\gamma+1}{3-\gamma} n'(i,0,t) \quad (78)$$

By continuity, and the fact that flow is choked in the orifice,

$$\frac{|u'(i-1, \Delta x(N+1), t)|}{a'(i,0,t)} = \frac{A_i}{A_{i-1}} \left(\frac{P'(i,0,t)}{P'(i-1, \Delta x(N+1), t)} \right)^{\frac{1}{\gamma}} \quad (79)$$

Using the isentropic relationship to get rid of $a'(i,0,t)$,

$$\frac{|u'(i-1, \Delta x(N+1), t)|}{a'(i-1, \Delta x(N+1), t)} = \frac{A_i}{A_{i-1}} \left(\frac{P'(i,0,t)}{P'(i-1, \Delta x(N+1), t)} \right)^{\frac{\gamma+1}{2\gamma}} \quad (80)$$

Using these equations with Eq. (16) and the definition of stagnation pressure,

$$\frac{P'_0}{P'} = \left\{ 1 + \frac{\gamma-1}{2} \left(\frac{u'}{a'} \right)^2 \right\}^{\frac{\gamma}{\gamma-1}} \quad (81)$$

one can obtain

$$\frac{|u'(i-1, \Delta x(N+1), t)|}{a'(i-1, \Delta x(N+1), t)} = \left\{ \frac{A_i}{A_{i-1}} \frac{2}{\gamma+1} + \frac{\gamma-1}{\gamma+1} \left(\frac{u'(i-1, \Delta x(N+1), t)}{a'(i-1, \Delta x(N+1), t)} \right) \right\}^{\frac{\gamma+1}{2(\gamma-1)}} \quad (82)$$

Given $m'(i-1, \Delta x(N+1), t)$, Eqs. (82) and (65) can be used to solve for u' , m' and a' . Since a closed form solution is not possible, the two equations must be solved iteratively. One should note that, because of the absolute values in Eq. (82) the flow direction is not explicit. Instead, it must be imposed in the same direction as the orifice flow (in this case, it will be negative).

The same equation can be used to solve for u' , a' and n' at point $(i+1, 0, t)$ by replacing the conditions at $(i, 0, t)$ with conditions at $(i, \Delta x(N+1), t)$, and replacing A_{i-1} with A_{i+1} . Analogous to Eq. (78), the upstream boundary of the orifice is defined by

$$n'(i, \Delta x(N+1), t) = \frac{3-\gamma}{\gamma+1} m'(i, \Delta x(N+1), t) \quad (83)$$

Although it is not explicitly stated, A_i can be a function of time, such as in a finite opening time valve or an ablative orifice (in which case, A_i could also be a function of integrated mass flow, temperature, etc.) The results of a constant versus variable area orifice is examined in subsequent sections.

5.3.3.4. Outflow

The final boundary condition concerns the downstream boundary of the entire system. If the flow is subsonic (this will occur for a very brief time prior to the choking of the orifice), the isentropic outflow condition will be governed by the exit pressure, which in this case, will be the lower pressure initially upstream of the diaphragm.

$$n'(i,0,t) = 2P'_{out} \frac{\gamma-1}{2\gamma} - m'(i,0,t) \quad (84)$$

The flow will be subsonic as long as

$$P'_{out} \geq \frac{(\gamma+1)a'^{\frac{2\gamma}{\gamma-1}} e^{-s'}}{2\gamma \left(\frac{u'}{a'}\right)^2 - (\gamma-1)} \quad (85)$$

a' , u' and s' can be evaluated at the point just upstream of the boundary, for reasons which will become apparent shortly.

If the right hand side of Eq. (85) rises above P'_{out} , the flow will become supersonic. In this case, all the characteristic lines are swept downstream, and no boundary condition is necessary, since all three characteristics can be found from the conditions at $(i, \Delta x, t)$. If the flow is supersonic just upstream of the boundary, at $(i, \Delta x, t)$, then the characteristics will slope downstream such that a solution can be found at the boundary. If the flow is subsonic, then the M' characteristic will slope upstream, and the subsonic condition will be needed to solve the boundary. This is why the supersonic condition is taken at one point upstream, rather than at the boundary itself.

6. Results

6.1. Similarity

It was shown earlier that, because of choking at the orifice, both the acoustic and flow pattern methods predicted that initial diaphragm pressure ratio, z , would not have an impact on the predicted pressure transmission. Before comparing results between all three methods, it is important to determine whether or not the Method of Characteristics demonstrates that same time dependence. Fig. 6.1 shows the solution for $z=100$ and $z=100000$, both for a 40% constriction ratio. When plotted versus non-dimensional time, $t'=ta_{ref}(L_{ref})^{-1}$, the pressure traces are identical, meaning that the solution is self-similar. Since the first two methods do not provide any time-dependent information, the Method of Characteristics can essential be considered z -independent and there is no need to compare the methods for different pressure ratios.

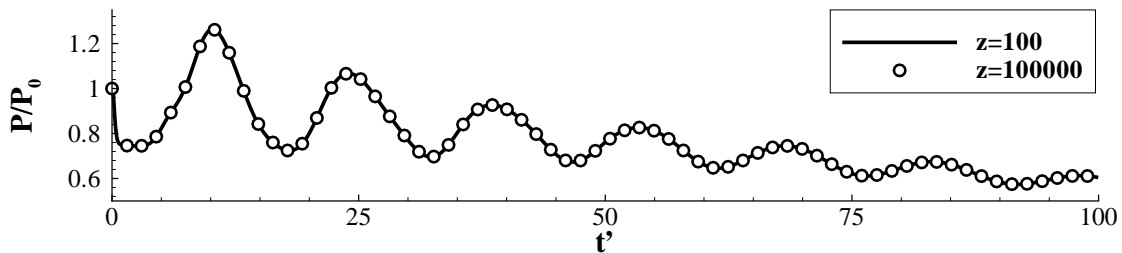


Fig. 6.1. Pressure histories in horizontal pipe for $z=100$ and $z=100,000$ with $C=40\%$

Nevertheless, the time scale of the problem is important. Some tunnels use perforated liners to relieve pressure to the outer tank. For a higher oscillation frequencies, this relieving mechanism will be more effective, because the pressures do not have to equalize as quickly. Furthermore, the higher the rate with which impact energy is added

to a material, the less energy is absorbed and converted to deformation, increasing the probability of brittle failure⁴. The liners are already in a very severe stress regime, since they are undergoing fluctuating multi-axial stresses. The shorter the timescale of the oscillations, the greater the likelihood of catastrophic failure.

From the definition of the nondimensional time, t' , the frequency of the problem will depend of the reference speed of sound, and the reference length. Therefore, as z increases, so will the frequency. Tunnel are more likely to fail at high values of z , not because of higher loading, but because it is experienced more rapidly. The inverse dependence on L_{ref} has implications for subscale modeling which may be conducted during the design process of full-scale facilities. Due to the nonlinear nature of the problem, one might expect additional wave interactions at small scale that, while validating the accuracy of the predictions methods, would not necessarily give useful information about a full-scale tunnel. The self-similarity implies that this is not the case, and experimental data from subscale models can be directly applied to the facilities on which they are based. However, it also means that, as transient start-up time is already very small for full-scale facilities, it will be even smaller for a model, necessitating a data-collection system with an extremely high sampling frequency and fast-response transducers.

6.2. Comparison of Solutions

Comparing the acoustic to the flow pattern method is very straightforward, since both methods generate a single value of pressure rise or fall for a given orifice size. The Method of Characteristics, however, provides an entire function of t and x for each value of C . Fig. 6.2-6.7 show pressure traces for $C=5\%$, 20% , 40% , 60% , 80% and 95% for the

horizontal and angled pipes, as well as the three sections of the heater. Pressure traces are taken at three x -locations for each pipe: the entry and exit boundaries and at the center. Predictions for incident and reflected pressures from the earlier two methods are plotted, as well.

For the horizontal pipe and the top and bottom sections of the heater, pressure is basically uniform across the entire length of the pipe at any given time (although for the horizontal pipe, the incident pressure wave can only be observed on the entry point.) For the angled pipe, the pressure exhibits the same general behavior across the pipe, but varies significantly in magnitude. In the midsection of the heater, pressure varies in magnitude and character across the length of the pipe. The explanation for such behavior is straightforward-- the horizontal pipe and the ends of the heater are each only "communicating" with one other pipe. The flow velocity at the other end is constrained in some way (0, in the case of the heater, and sonic for the horizontal pipe). Pressures in the angled pipe and the middle of the heater are being driven by varying states at both ends, which leads to significant variations in pressure with x . For the angled pipe, the pressure trace in the downstream end of the pipe will resemble the pressure trace in the horizontal pipe. The pressure trace in the upstream end will resemble the pressure trace on the downstream ends of the top and middle of the heater. In turn, the upstream end of the middle pipe will resemble the bottom of the heater.

These pressure variations over x make it difficult to compare the quasi-steady predictions with the Method of Characteristics. Compounding this problem is the unsteady nature of the Method of Characteristics solution. In some of the traces, distinct minima are present providing obvious comparison values. However, these minima may

not always be distinguishable. As an example, consider the horizontal pipe; the incident wave is a rarefaction. The horizontal pipe leads to an area contraction at the angled pipe, so the wave reflected from that junction is also a rarefaction. Therefore, the incident wave will not form a minimum, but, in a best case, a plateau, and in the worse case, a line which passes through that point. In fact, for the case of the horizontal pipe, a plateau will be seen in the pressure trace at the downstream boundary, but at any upstream value of x , it will be absorbed into the reflected rarefaction. Now consider the angled pipe; in this case, the incident wave is a rarefaction, and the reflected wave is a compression. The incident wave will form a distinct minimum, and theoretically, the reflected wave should generate a maximum. This is not the case. Instead, the reflected wave forms a small plateau (if at all; at the upstream boundary, the incident and reflected waves merge together into a single minimum), then rises to an overpressure not predicted by either quasi-steady method. Upstream of the angled pipe, the transmitted rarefaction through the heater middle reflects off the area change in the heater. As it travels downstream, it is intensified by the junction with the angled pipe (since the wave is now traveling downstream, it sees this junction as an area reduction). One could generate further acoustic predictions on this phenomena, but without adding some sort of time dependence, it would be difficult to determine which waves to add together. A time-dependent acoustic method would not be difficult to implement computationally, but if so much computation effort were to be put in, the Method of Characteristics would be a better choice.

For the heater bottom, the incident and reflected waves are so close together that the graph more closely resembles a linear decrease in pressure than an oscillation. At the

downstream junction, plateaus can be distinguished, but for all practical purposes, this prediction would have little value in determining loads on structural members. For this case, it is fortunate that pressure changes in the bottom of the heater are very small and gradual in comparison to changes in the more upstream pipes. The bottom portion of the heater can be designed safely to the specifications of the rest of the apparatus.

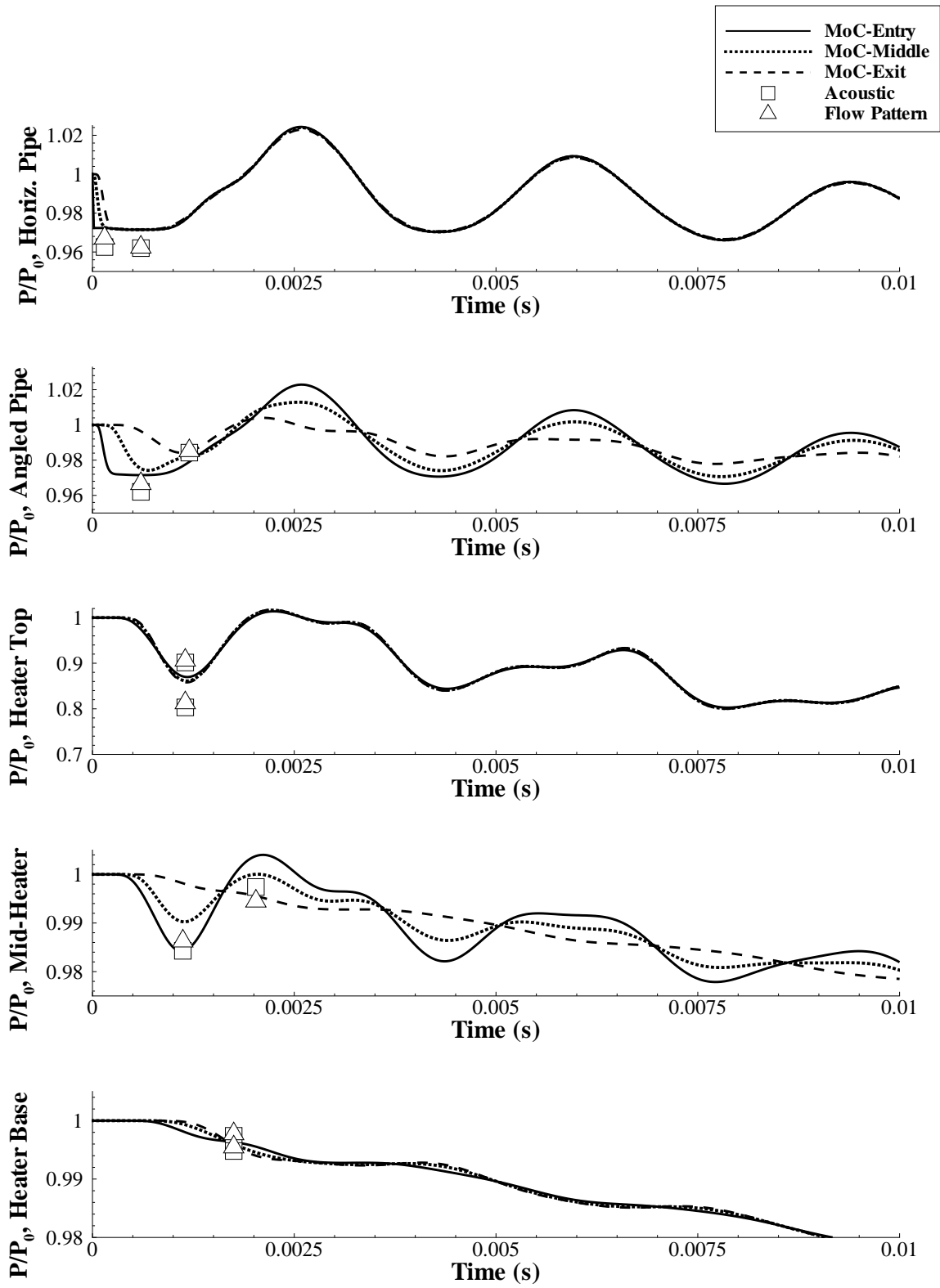


Fig. 6.2. Pressure traces for $C=5\%$

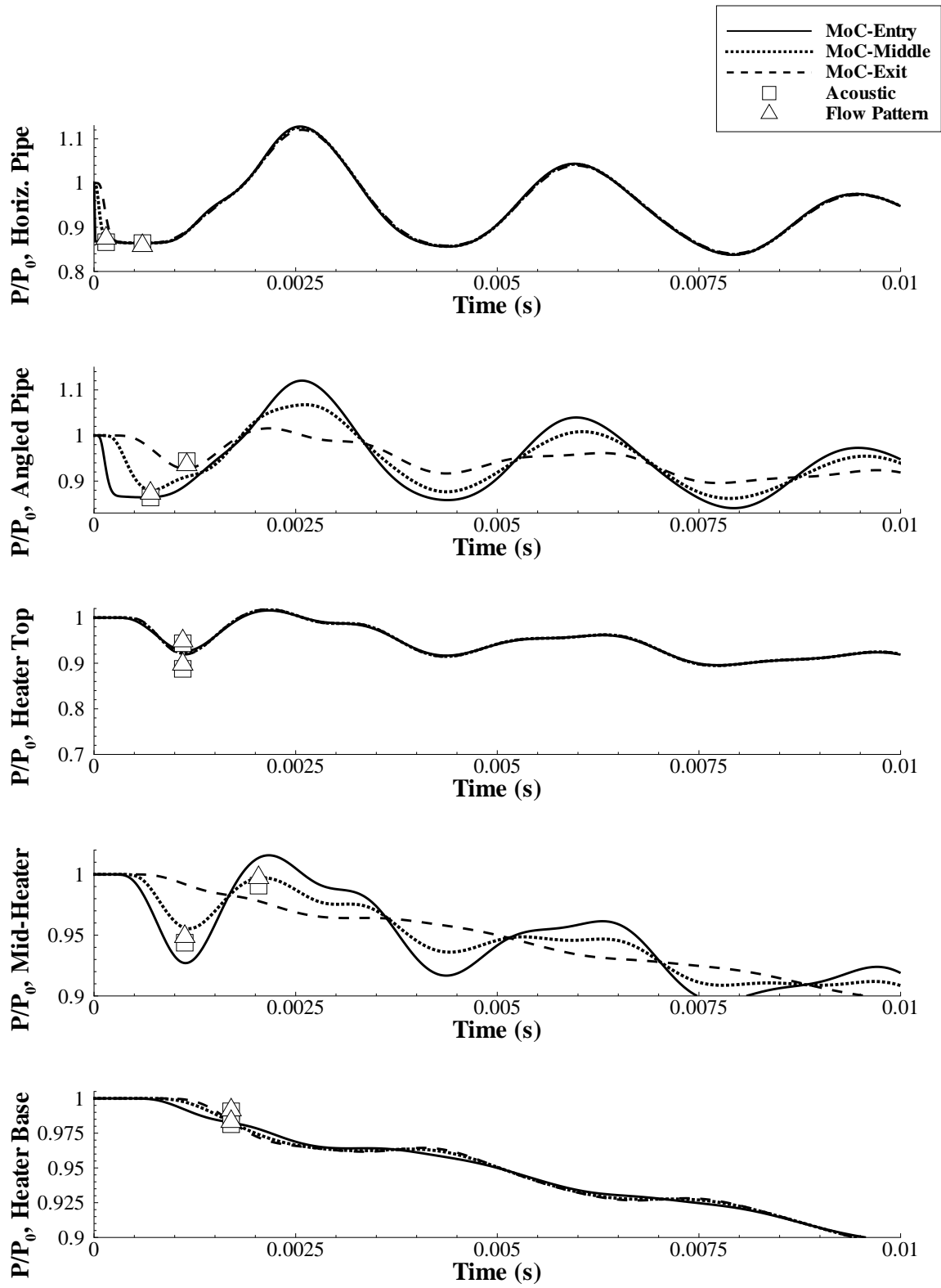


Fig. 6.3. Pressure traces for $C=20\%$

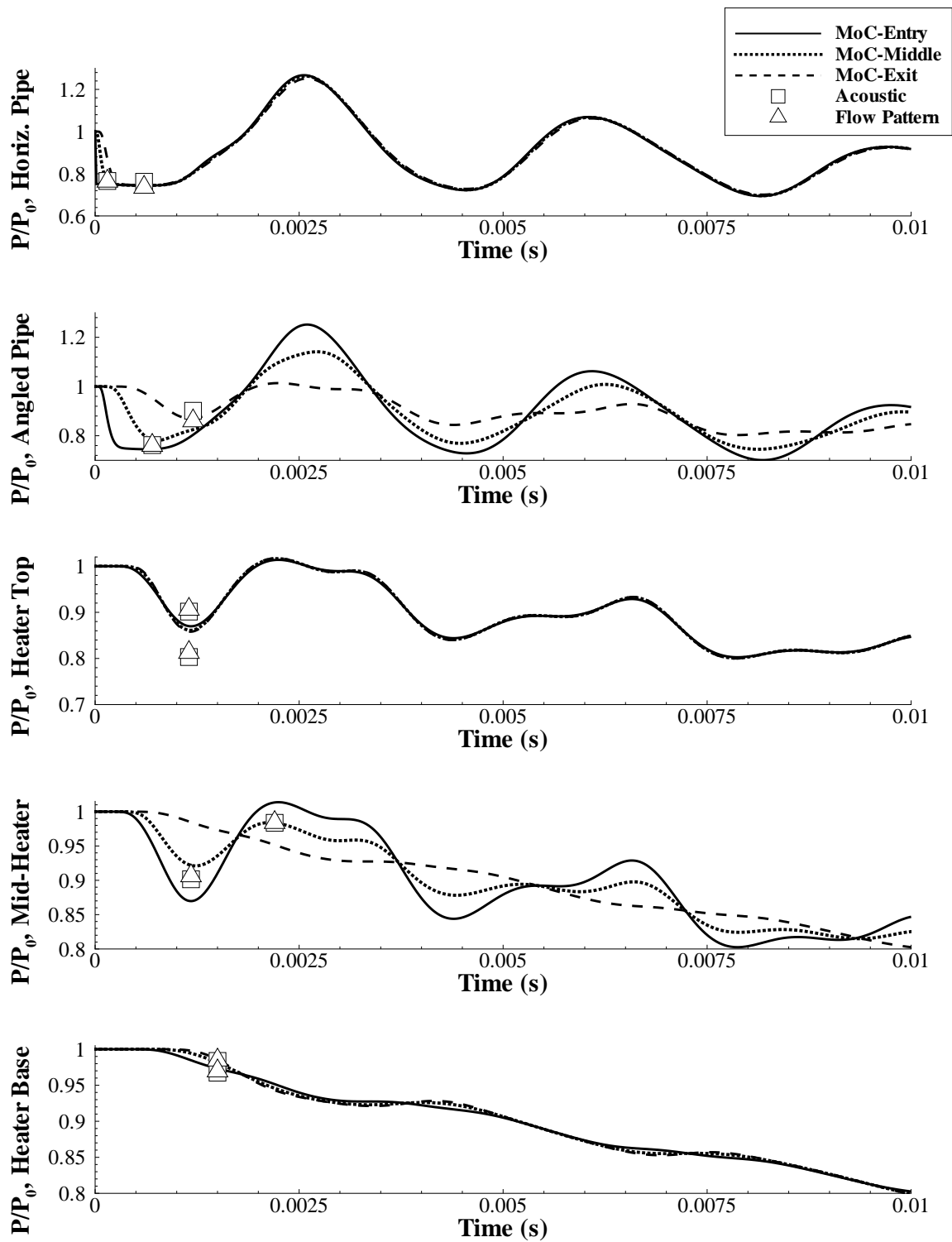


Fig. 6.4. Pressure traces for $C=40\%$

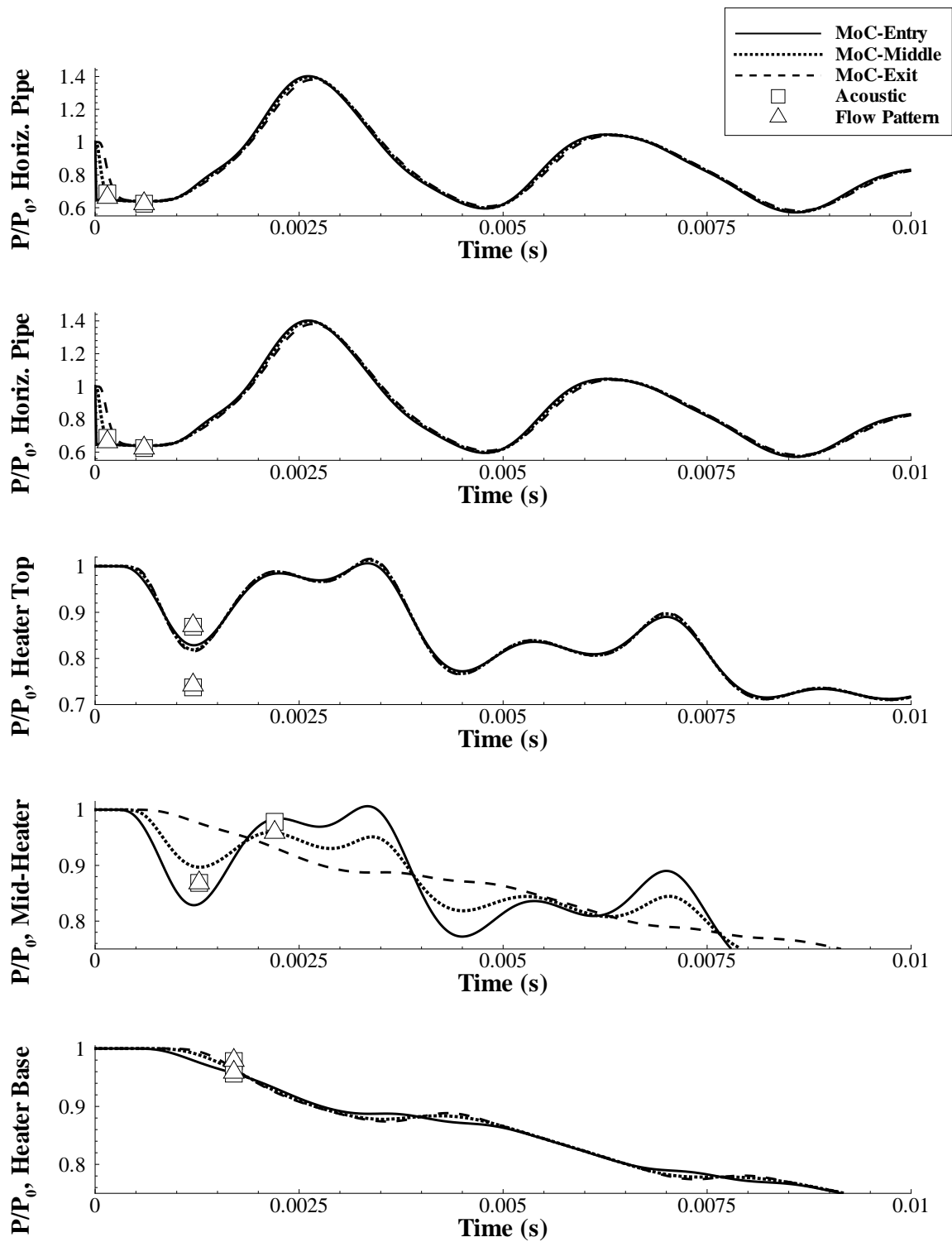


Fig. 6.5. Pressure traces for $C=60\%$

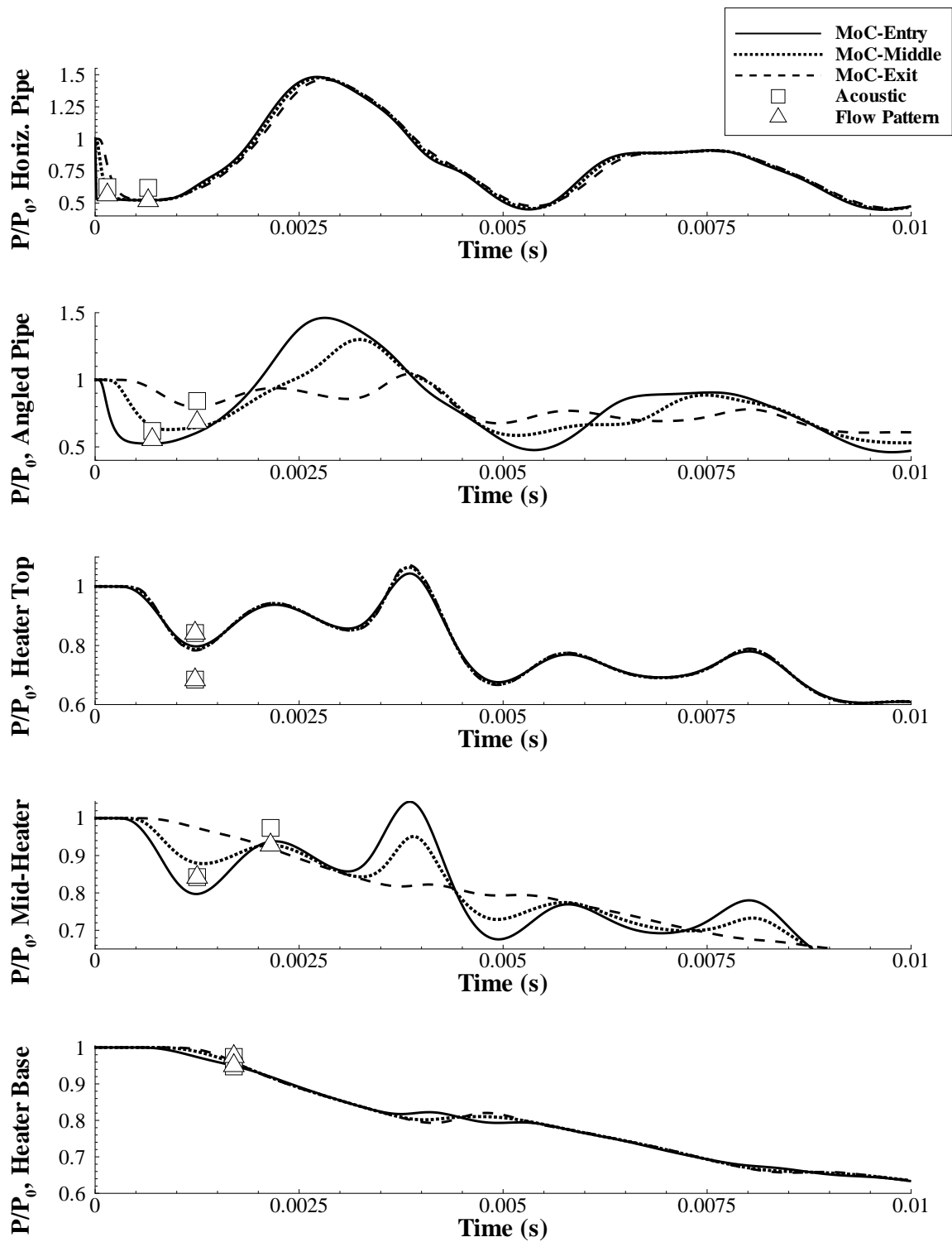


Fig. 6.6. Pressure traces for $C=80\%$

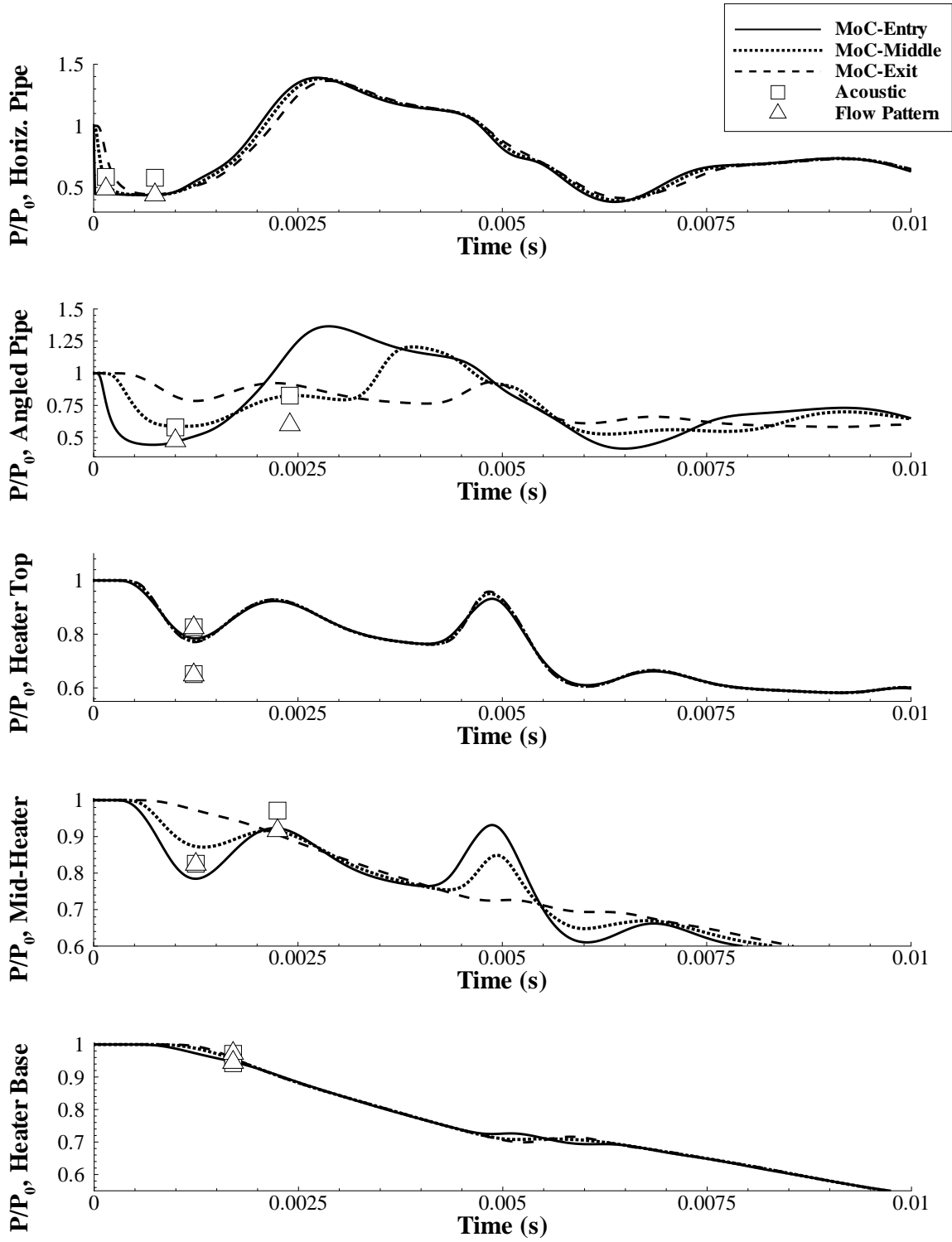


Fig. 6.7. Pressure traces for $C=95\%$

Fig. 6.8a-h shows raw comparisons of the three methods, where the results with Method of Characteristics are taken as the appropriate maximum, minimum or plateau, as discussed. For the top of the heater, there is only a single relevant pressure drop, which is compared to both the incident and reflected predictions from the acoustic and flow pattern methods. For the bottom of the heater, as discussed above, there are no significant minima, although plateaus can be distinguished near the entry if C is very small. Instead of taking actual plateaus, the quasi-steady methods are compared to characteristics solutions at the time value for which this plateau is located (for this example, $t=.0017s$). From the locations of the various minima in other pipes, it can be seen that the locations of the various flow structures vary only slightly in time with different values of C . The upstream boundary of the middle pipe is found in a similar manner, except that since there are visible minima and maxima at the center of the pipe, for each value of C , the pressure at the exit is evaluated slightly after the time location of the minimum at the midpoint, and slightly after the time location of the maximum. (The offset is based on the difference in time locations of the minima and maxima at the midpoint and entry of the pipe.)

For the horizontal pipe (Fig. 6.8a-b), the flow pattern method closely matches the Method of Characteristics over the entire range. The acoustic method matches well for small values of C , beginning to deviate around $C=40\%$. For small values of C , the pipe is much larger than the orifice, so the Mach number in the pipe will be much less than one, meaning that the flow will be nearly incompressible. As C rises, so does the Mach number in the pipe, and the assumption of incompressibility becomes less and less appropriate.

In the angled pipe (Fig. 6.8c-d), pressure varies significantly with x . For the incident wave, the flow pattern method gives a close approximation of the pressure at downstream end of the pipe. The acoustic method, on the other hand, gives a good approximation at the middle of the pipe. Neither method approximates flow at the upstream end. In contrast, for the wave reflected from the heater junction, the acoustic method gives good results on the upstream end of the pipe. The flow pattern method matches the upstream values for small values of C , and the middle values for larger values of C . Here, neither method matches the downstream reflections.

For the middle of the heater, (Fig. 6.8e-f), pressure is roughly uniform through the pipe for small values of C , with agreeable results from the quasi-steady methods. As C increases, it can be observed that the changes in pressure across the pipe become more significant. In this case, the quasi-steady methods give very similar results, which do not match conditions at any of the sampled points in the pipe, but are roughly half-way between the midpoint values and the upstream values. For the reflected wave, the pressures behave very nonlinearly in C , a trend which is not captured by either quasi-steady solution. The flow pattern and acoustic solutions generally approximate the flow on the upstream half of the pipe for low values of C , but otherwise, do not match well for this portion of the heater.

For the top and bottom of the heater (Fig. 6.8g-h), the opposite occurs. The incident and reflected quasi-steady approximations generate an envelope around the Method of Characteristics solutions. For small values of C , this envelope is small, and the solutions match well. However, as C increases, the envelope diverges, until for $C=95\%$, it spans about 20% of the stagnation pressure. For the top of the heater, the Method of

Characteristics solutions tend slightly toward the incident prediction, whereas for the bottom, they tend more towards the reflected predictions.

In general, between all the pipes in the system it has been found that the quasi-steady methods are, as a whole, far more accurate for small values of C . Furthermore, when C is small, there is little difference between the flow pattern method and the acoustic method. The acoustic method is far easier to implement, and can be iterated if one wished to attempt to predict the reflected overpressures. However, at least in the case of the horizontal pipe, the flow pattern method gave good matching to higher values of C than the acoustic method. In general, the quasi-steady methods did not appear to correspond to any particular axial location, although in comparison to experiment, one might expect that the approximations would be more inaccurate in the vicinity of the stepped area change section, since separation at the corners of the area change would decrease the effective flow area. Although it is easy to match the quasi-steady results to the Method of Characteristics results, the quasi-steady results by themselves may or may not be useful in the ultimate goal of predicting the stress loading on the structural members.

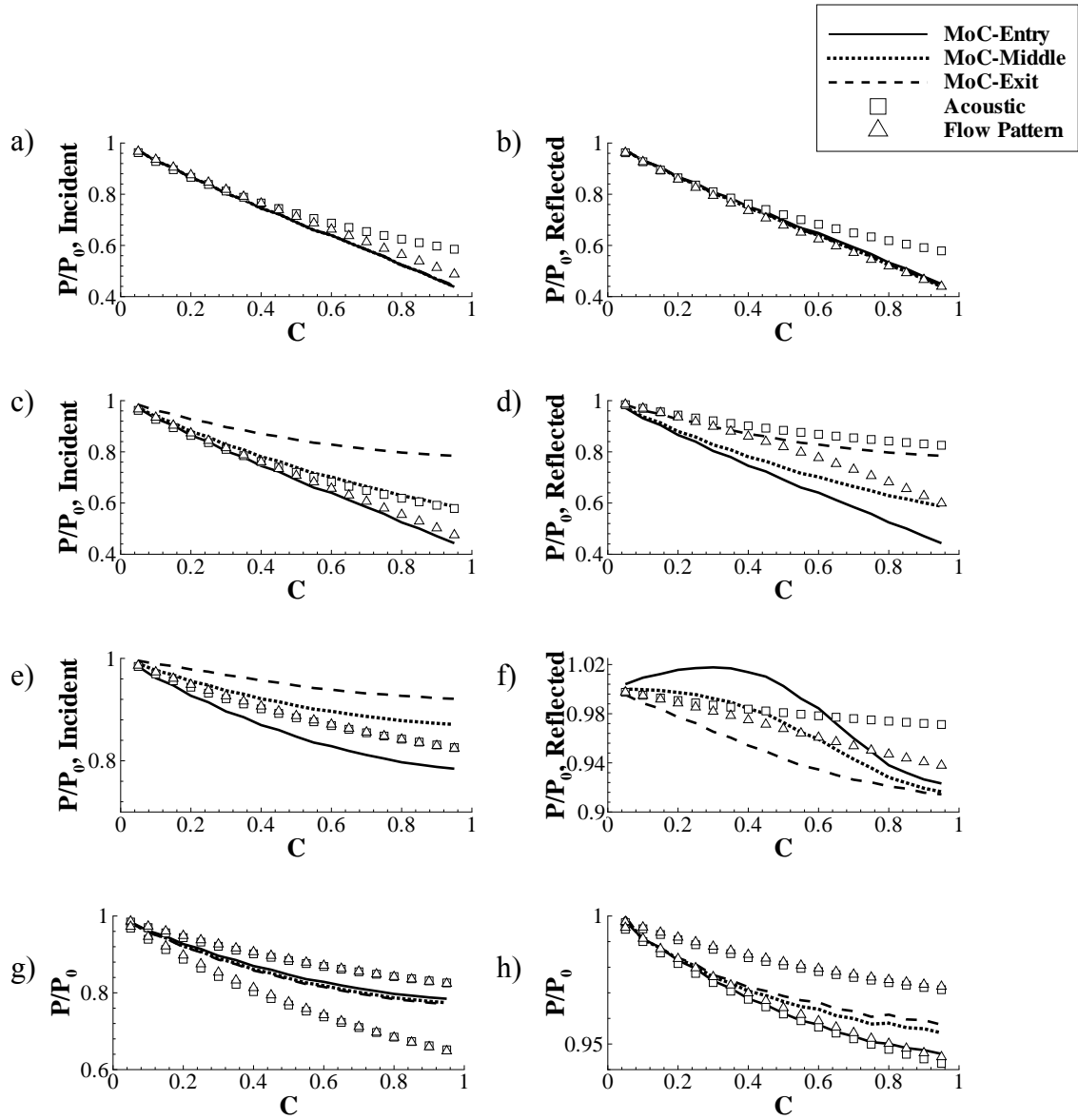


Fig. 6.8. Comparison of pressure predictions between methods. a-b) Incident and reflected waves, horizontal. c-d) Incident and reflected waves, angled pipe. e-f) Incident and reflected waves, middle of heater. g) Top of heater. h) Bottom of heater.

6.3. Application to Tunnel Design

This investigation into quantifying transient pressure drop was motivated by the desire for an improved design tool. This tool can be used in two ways. For an existing tunnel, one can determine the orifice size necessary to prevent excessive loading on tunnel components. Alternately, it could be used to determine performance requirements for a new facility. The results of this method provide three useful pieces of data: maximum pressure magnitudes, spatial pressure gradients, and temporal pressure gradients.

Assume that one wishes to design a pebble bed heater using alumina pebbles, as in an example given by Pope.³⁴ Alumina has a density of approximately 37.7 kN/m^3 . Assuming 33% porosity, the pebbles have a bulk density of 25.1 kN/m^3 . Now, assume the supply pressure of the heater is 10 MPa, which is a modest, but reasonable value for a hypersonic tunnel. In order to prevent the pebbles from lifting, the pressure gradient in the tunnel cannot be greater than 25.1 Pa/m , or 0.25% of the supply pressure per meter. Using the Method of Characteristics, one could calculate the pressure gradient across the lower tank of the heater, as shown in Fig. 6.9 for $C=40\%$. Here, the maximum pressure gradient is about 1.5%/m, which means that one would need to use either a smaller orifice or more dense pebble material to prevent pebble lift.

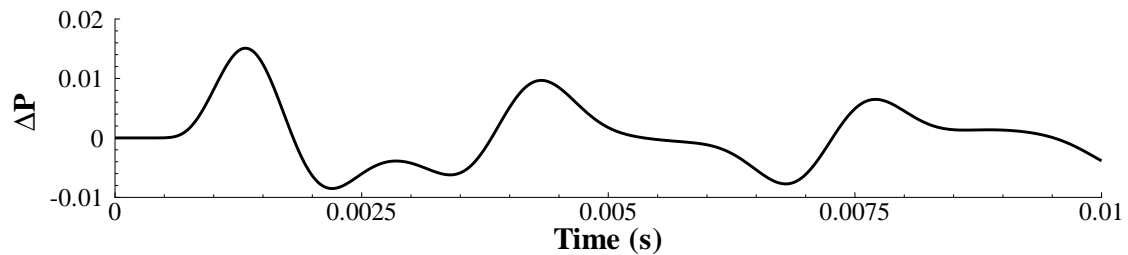


Fig. 6.9. Pressure drop across the heater base.

Pressure gradients in time can also be used as design parameters. Suppose one is using perforated liners capable of venting up to 500 MPa/s. Assume that one would like to run at a pressure ratio of 10,000, using an orifice with 40% constriction, but there is concern about crushing the top liner. Referring to Fig. 6.4, these values of z and C will result in a 15% pressure drop over .001s. Again, using 10MPa as the supply pressure, this means that inside the liners, the pressure will drop by 1.5MPa, but outside the liners, it will only drop by .5 MPa, generating a 1.0 MPa compressive force on the liners. Stress on a pressure vessel is given by

$$\sigma = \frac{rP}{t} \quad (86)$$

Using the dimensions of the model tunnel, r at the top is 0.188 m. Therefore, $\sigma = 188$ MPa m. Depending on the yield strength of the liner material, the required thickness of the liners can be determined. Alternately, designing for a "worst case" scenario, one could choose σ based on the maximum pressure drop of 1.5 MPa.

These are two highly simplified cases where pressure gradients in time and space can be used as inputs for design functions. In reality, the venting ability of the liners will rarely be constant, and is likely to depend on the thickness. More refined values of the spatial gradient across the pebble bed could be taken using all of the grid points, instead of just the top and bottom. Nevertheless, it has been demonstrated that these analyses can provide useful inputs for failure prediction methods as well as design procedures for new facilities.

6.4. Ablative Orifice

One unparalleled advantage of the Method of Characteristics over the quasi-steady methods is the ability to include distinctly time-dependent effects. Finite-time opening orifices have been used to expand the useful test time of shock tubes^{26,30}, and may also be useful in a situation where the orifice size needed to protect the upstream components is too small to permit the necessary mass flow for desired test conditions.

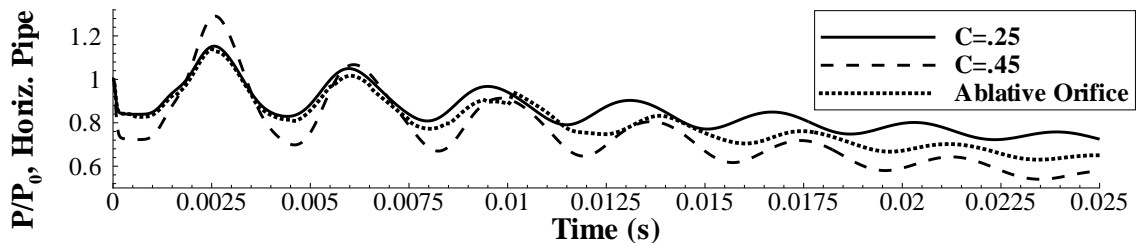


Fig. 6.10. Pressure traces in horizontal pipe for $C=.25$, $C=.45$ and a variable area orifice which expands from $C=.25$ to $C=.45$ over the first .01s (shown at axial midpoint of pipe).

Error! Reference source not found. shows the pressure trace in the horizontal pipe for an orifice which initially has $C=25\%$, and then expands linearly in time to 45% over .01s. Results for constant area cases where $C=25\%$ and 45% are shown for comparison. Intuitively, one might assume that the solution would initially resemble the constant area $C=25\%$ solution, and after $t=.01$ s, resemble the constant area $C=45\%$ solution. To some degree this is correct: at very small times, the solution is identical to the constant area 25% case. As time increases, it tends towards the 45% case, but the solutions are not identical. The variable-area orifice generates a much shallower oscillation which has approximately the same peak value as for the constant area $C=45\%$,

but the valleys are not as deep. This could imply that a variable-area valve would have the additional benefit of reducing the severity of the loading on the heater tank, although a more comprehensive study would need to be done. Furthermore, the quasi-steady methods have no way of predicting or modeling such behavior, meaning that the Method of Characteristics or some other time-dependent method is essential in characterizing this behavior.

7. Design of Experiment

Based on the trends observed from the three methods examined in this study, a subscale validation experiment has been designed in conjunction with AEDC Hypervelocity Tunnel 9. The geometry of the test article has been modeled after the geometry of Tunnel 9 (not shown for proprietary reasons) at roughly one-quarter length scale. Analytical pressure predictions for this model have been generated using the general methodology demonstrated above. The walls of the test article will be over-designed to withstand the large pressure oscillations. One of the assumptions which most heavily governs the behavior of the models shown above is that of choked orifice flow. If the experimental flow pattern is dependent on z , all of the demonstrated methods are invalidated, in which case, either a correction function must be included in the procedure, or alternative methods must be investigated. The "heater" of the article will be filled with unheated, pressurized nitrogen. Flow will be induced via the bursting of a double-diaphragm. For lower values of z , the flow will exhaust to atmospheric pressure. To achieve higher pressure ratios, the test apparatus will be attached to a vacuum line. The highest z achieved with atmospheric pressure will overlap the smallest z achieved with the vacuum line to ensure that decreasing the exit pressure is equivalent to increasing the heater pressure. In this manner, values of z ranging from 10 to 15,000 will be investigated, which greatly expands the existing envelope of experimental results, which range from slightly above 1 to 1000.^{1,8,40}

The orifice plate of the apparatus will be removable, so that multiple values of C can be tested. These values will be focused on "realistic" orifice sizes, rather than the full range of values presented above. Rarely would it be necessary to constrict the flowpath to

a pinhole opening, nor to insert an orifice which barely changes the effective area of the flow. Orifices will be machined to provide values of $C=14.5\%$, 17.0% , 25.4% , 31.3% and 54.7% . (It should be noted that most of these "realistic" constriction values are mainly in the region where the quasi-steady methods showed good agreement with the Method of Characteristics for the original model considered). Orifices of other C values or other geometries (multiple holes, square openings, etc) could later be machined if further experiments were desired.

As explored above, the results gained from the subscale model should be directly applicable to Tunnel 9 itself, on a slower time-scale. Seven pressure transducers will be placed at points in the tunnel to provide information relating to individual pressure drop in each pipe, axial variation of pressure conditions and two-dimensional effects. Data will be collected by a multi-channel, high-speed data system at a frequency of 500kHz , or once every $2\mu\text{s}$, which, based on the method of characteristic predictions, should be appropriate to accurately capture the oscillatory nature of the pressure behavior.

8. Conclusions

The purpose of this study has been to investigate three possible methods of predicting the transient pressure behavior caused by the starting process of a hypersonic blow-down tunnel. One method, the Flow Pattern Assumption Method, was introduced in this study using combination of existing methods which had not before been used in conjunction. In addition, comparing the results of methods based on different assumptions has granted some insight on the important features of the flow.

Revisiting Section 2, a number of the features were initially assumed to be critical to the flow. From the results of the three analyses, some different conclusions can be drawn. Although the problem may include large pressure ratios, due to choking at the orifice, these pressure differences are limited to the region upstream of the orifice. Some of the inaccuracies associated with the large pressure ratios, such as imperfect diaphragm rupture, may still affect the problem, but experimental validation will be necessary to address such issues. Furthermore, the induced flow velocities are subsonic, and for small values of C , are so small that the flow is essentially incompressible. Although extreme gas temperatures mean that γ is a function of T , if ρ is constant and Δp is small (as in the case for small orifices and upstream pipes) T will be roughly constant, and thus, so will γ .

In contrast, the time-dependence does play an important role in the process. Although the quasi-steady methods could usually successfully approximate important minima and maxima, certain wave interactions could not be predicted without time-dependence. The pressure behavior with time was inherently different for each pipe in the system. Although the behavior was primarily oscillatory, some pipes experienced overpressures while others did not, and the heater bottom experienced a nearly linear

pressure drop. An orifice with time-varying area created a distinctly different pressure pattern than one of constant area. Furthermore, time-dependent structural loading is inherently different than steady loading, which means that time-dependent pressure traces are necessary in order to accurately predict the stresses.

In Section 2, a number of desirable model qualities were defined. The first was simplicity. The acoustic method is the simplest of those explored-- it can be performed by hand and since it is linear, additional reflections can be computed and superposed. The flow pattern method is conceptually elegant, and can be solved using software with packaged root-finders, but the derivation is long-winded and it cannot be solved by hand. The Method of Characteristics is fairly straightforward, but requires far more coding than the other two methods.

All three methods are modular. Each junction or boundary is treated individually. In fact, their modularity is demonstrated in the way weaknesses in one method may be overcome using results from another method. The flow pattern method has no mechanism for handling solid boundaries, but because of the modularity, the methods can be interchanged, and an acoustic reflection can be applied to a rarefaction generated by the flow pattern method. The choking condition which is absolutely critical to the acoustic method is taken from the flow pattern method. Many of the boundary conditions in the Method of Characteristics are identical to those in the acoustic method. In addition, all three solutions are non-dimensional.

The final criterion is accuracy. Since no experimental data is yet available for comparison, it is difficult to make a judgment on the absolute accuracy of any of the methods. Nevertheless, some educated guesses can be made, based on knowledge of the

methods' respective derivations. The flow pattern and acoustic method generate very similar solutions whenever C is small, occasionally when it is large. The flow pattern method incorporates more accurate approximations of the flow structures, but the similarity of the results implies that the assumptions made by the acoustic method are often acceptable. Since the acoustic method is so much simpler to implement than the flow pattern method, for cases of small C , it should be chosen over the flow pattern method. The agreement between all three methods is generally good, being very accurate in portions of the tunnel, and varying by significant fractions of the stagnation pressure in others. Most of this inaccuracy can be traced to the fact that the quasi-steady methods provide a single point of data, while the Method of Characteristics generates a two-dimensional function of data. If one considers the axial midpoint of each pipe, the quasi-steady methods will generate an acceptable approximation for the first pressure drop as long as C is less than about 40-50%.

It is obvious that the amount of information provided by the Method of Characteristics outstrips the data provided by the other methods. To fully understand the nature of the pressure behavior during startup, the Method of Characteristics is essential. It provides general time scale as well as frequency of oscillation, and provides all of the pressure extrema instead of one or two. Time dependent analyses, such as for time-dependent area orifice and vented liners can be considered. There is no need to guess where solutions are applicable, because a more robust set of data is provided. If the flow through a given facility is well understood and a quick and simple pressure drop provider is necessary, the acoustic method may be a better choice. However, it is still useful to compare the acoustic method to the Method of Characteristics for a given tunnel

geometry to ensure that it is within acceptable bounds of accuracy. In short, although Method of Characteristics is a computational, rather than closed form solution, it is relatively straightforward to program, and the amount of data it provides is well worth the initial coding investment.

BIBLIOGRAPHY

1. Alpher, R. A. and White, D. R., "Flow in shock tubes with area change at the diaphragm section," *Journal of Fluid Mechanics*, Vol. 3, No. 2, 1958, pp. 457-470.
2. Amann, H. O., "Experimental Study of the Starting Process in a Reflection Nozzle," *The Physics of Fluids Supplement I*, No. 12, 1969, pp. I-150-I-153.
3. Anderson, J. D., *Hypersonic and High Temperature Gas Dynamics*, AIAA, Reston, 2000.
4. Askeland, D., *The Science and Engineering of Materials*, 3rd Ed., PWS Publishing Company, Boston, 1994.
5. Baals, D. and Corliss, W., *Wind Tunnels of NASA*, National Aeronautics and Space Administration, Washington, D.C., 1981.
6. Barbour, N. and Imrie, B., "A Reservoir/Orifice Technique for Extending the Useful Running Time of a Ludweig Tube," *Modern Developments in Shock Tube Research: Proceedings of the Tenth International Shock Tube Symposium*, Shock Tube Research Society, Japan, 1975, pp.252-259.
7. Benedict, R., Carlucci, N. and Swetz, S., "Flow Losses in Abrupt Enlargements and Contractions," *ASME Journal of Engineering for Power*, Vol. 88, January 1966, pp .67-72.
8. Britan, A. B., Vasil'ev, E.I. and Mitichkin, S., "Wave Processes in a Shock Tube of Variable Cross-Section," *High Temperature*, Vol. 30, No. 6, Nov/Dec 1992, pp. 939-943.
9. Chorin, A., "Random Choice Solution of Hyperbolic Systems," *Journal of Computational Physics*, Vol. 22, 1976, pp. 517-533.
10. Courant, R. and Friedrichs, K.O., *Supersonic Flow and Shock Waves*, Interscience Publishers, Inc., New York, 1948.
11. Gaydon, A. G., and Hurlle, I. R., *the Shock Tube in High-Temperature Chemical Physics*. Reinhold Publishing Corporation, New York, 1963.
12. Glimm, J., "Solution in the Large for Nonlinear Hyperbolic Systems of Equations," *Communications in Pure and Applied Mathematics*, Vol. 18, 1965, pp. 697-715.

13. Gottlieb, J. J. and Igra, O., "Interaction of Rarefaction Waves with Area Reductions in Ducts," *Journal of Fluid Mechanics*, Vol. 137, December 1983, pp.285-305.
14. Hall, J. G. and Russo, A. L., "Simplification of the Shock-Tube Equation," *AIAA Journal*, Vol. 1, No. 4, April 1963, pp. 962-963.
15. Hunter, J., *Acoustics*. Prentice-Hall, Inc., Englewood Cliffs, 1962.
16. Igra, O. and Gottlieb, J.J., "Interaction of Rarefaction Waves with Area Enlargements in Ducts," *AIAA Journal*, Vol. 23, No. 7, 1983, pp.1014-1020.
17. Igra, O. Wang, L. and Falcovitz, J. "Non-Stationary Compressible Flow in Ducts with Varying Cross-Section," *Proceedings of the Institution of Mechanical Engineers, Part G - Journal of Aerospace Engineering*, Vol. 212, No. 4, 1998, pp.225-243.
18. Jacobs, P.A., "Numerical Simulation of Transient Hypervelocity Flow in an Expansion Tube." NASA Contractor Report 189615, ICASE Report No. 92-10. March 1992.
19. Kaneko, M. and Nakamura, Y. "Effects of Shock Wave/Boundary Layer Interaction on Reservoir Temperature in Shock Tunnel," AIAA 99-3529.
20. Kashimura, H., Iwata, N. and Nishida, M., "Numerical Analysis of the Wave Propagation in a Duct with an Area Change by Random Choice Method." *Bulletin of JSME*, Vol. 29, No. 251, May 1986, pp. 1440-1445.
21. Kinsler, L. and Frey, A., *Fundamentals of Acoustics, 2nd Edition*. John Wiley & Sons, New York, 1962.
22. Kentfield, J., *Nonsteady, One-Dimensional, Internal, Compressible Flows: Theory and Applications*. Oxford University Press, Inc., New York, 1993.
23. Lee, J. and Lewis, M., and Diewert, G., "Numerical Study of Flow Establishment Time in Hypersonic Shock Tunnels," *Journal of Spacecraft and Rockets*, Vol. 30, No. 2, 1993, pp.152-163.
24. Liepmann, H. W. and Roshko, A., *Elements of Gas Dynamics*, Dover Publications, New York, 1957
25. Majanovic, P. and Djordjevic, V., "On the Compressible Flow Losses Through Abrupt Enlargements and Contractions," *ASME Journal of Fluids Engineering*, Vol. 116, Dec. 1994, pp.756-762.
26. Matsuo, K., Kawagoe, S. and Ogawara, T., "Experimental Studies of a Supersonic Ludwieg Tube with an Upstream Valve," Barbour, N. and Imrie, B., "A Reservoir/Orifice Technique for Extending the Useful Running Time of

- a Ludweig Tube," *Modern Developments in Shock Tube Research: Proceedings of the Tenth International Shock Tube Symposium*, Shock Tube Research Society, Japan, 1975, pp.265-272.
27. Matsuo, K., Kawagoe, S., Kage, K. and Araki, K., "Choking Phenomena of Flows in a Shock Tube," *Bulletin of the JSME*, Vol. 20, No. 144, June 1977.
 28. Matsuo, K., Kawagoe, S. and Ogawara, T., "Starting Process of a Supersonic Ludwieg Tube with a Downstream Valve," *Bulletin of the JSME*, Vol. 21, No. 161, November 1978, pp.1610-1617.
 29. Matsuo, K., Kawagoe, S., Mizuma, M. and Kondoh, N., "Extension of the Steady Flow Duration of a Ludwieg Tube using a Reservoir-Orifice Method: Part I. Case of Orifices with Fixed Opening Area," *Bulletin of the JSME*, Vol. 22, No. 163, January 1979, pp.718-724.
 30. Matsuo, K., Kawagoe, S., Mizuma, M. and Kondoh, N., "Extension of the Steady Flow Duration of a Ludwieg Tube using a Reservoir-Orifice Method: Part II. Case of Orifices with Variable Opening Area," *Bulletin of the JSME*, Vol. 22, No. 173, November 1979, pp.1554-1561.
 31. Morton, K.W. and Mayers, D. F., *Numerical Solution of Partial Differential Equations*, Cambridge University Press, Cambridge, 1994.
 32. Murty, H. S. and Gottlieb, J. J., "Analytical and Numerical Study of the Flow in a Shock Tube with an Area Change at the Diaphragm Section." UTIAS Technical Note N. 255.
 33. Paull, A. and Stalker, R. J., "Test Flow Disturbances in an Expansion Tube." *Journal of Fluid Mechanics*, Vol. 245, 1992, pp. 493-521.
 34. Pope, A. and Goin, K. *High-Speed Wind Tunnel Testing*. John Wiley & Sons, Inc., New York, 1965.
 35. Resler, E. L., Lin, S. C. and Kantrowitz, A., "The Production of High Temperature Gases in Shock Tubes," *Journal of Applied Physics*, Vol. 23, No. 12, 1952, pp.1390-1399.
 36. Russell, D.A., "Orifice Plates in a Shock Tube." *Physics of Fluids*, Vol. 5, No. 4, 1962, pp. 499-500.
 37. Rudinger, G., *Wave Diagrams for Nonsteady Flow in Ducts*, D. Van Nostrand Company, Inc., New York, 1955.
 38. Saito, T. and Glass, I., "Application of Random-Choice Method to Problems in Gas Dynamics," *Progress in Aerospace Sciences*, Vol. 21, pp. 201-247. 1984.

39. Sod, G. A., "A Numerical Study of a Converging Cylindrical Shock," *Journal of Fluid Mechanics*, Vol. 83, Part 4, 1977, pp.785-794.
40. Sugiyama, H. "Performance Study of Shock Tubes with Area Change at the Diaphragm Section," *Bulletin of the JSME*, Vol. 26, No. 216, June 1983. pp. 958-963. Paper No. 216-6.
41. Swaffield, J. A. and Boldy, A. P., *Pressure Surge in Pipe and Duct Systems*. Avebury Technical, Brookfield, VT, 1993.
42. Toro, E. F. "A New Numerical Technique for Quasi-Linear Hyperbolic Systems of Conservative Laws," CoA Report No. 86/26, December 1986, College of Aeronautics, Cranfield Institute of Technology, Cranfield, Beds, England.
43. Toro, E. F. and Roe, P.L., "A Hybridised Higher-Order Random Choice Method for Quasi-Linear Hyperbolic Systems," *Shock Tubes and Waves: Proceedings of the 16th International Symposium on Shock Tubes and Waves, Aachen, West Germany, July 26-31, 1987*, edited by H. Grönig, Rheinisch-Westfälische Technische Hochschule Aachen, 1987.
44. White, F. M., *Viscous Fluid Flow*, 2nd ed., McGraw-Hill, Boston, 1991.